RSC Advances

ROYAL SOCIETY OF CHEMISTRY

www.rsc.org/advances

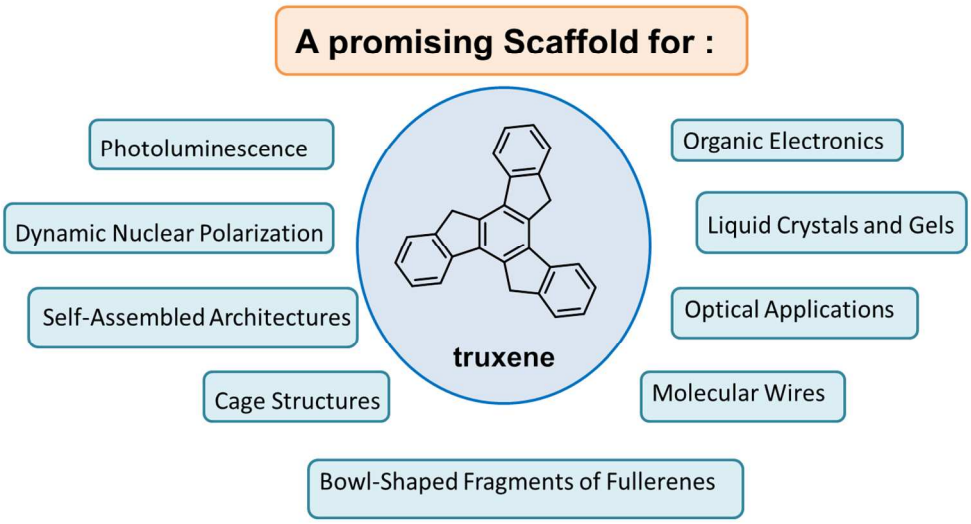

Graphical Abstract
246x142mm (150 x 150 DPI)

RSC Advances

RSCPublishing

ARTICLE

Truxene: a Promising Scaffold for Future Materials

Cite this: DOI: 10.1039/xoxxoooooox

Fabrice Goubard*[a] and Frédéric Dumur*[b]

Received ooth January 2012,
Accepted ooth January 2012

DOI: 10.1039/xoxxoooooox

www.rsc.org/

Truxene (10,15-dihydro-5*H*-diindeno[1,2-*a*;1',2'-*c*]fluorene), which is a heptacyclic polyarene structure, has attracted a great deal of interest due to its exceptional solubility, high thermal stability and ease with which it may be modified. Over the years and thanks to the advances in the synthesis of truxene derivatives, the scope of applications of this attractive building block initially limited to synthesis and photoluminescence has been nowadays extended to Organic Electronics. This review aims at highlighting the benefits brought by the introduction of this rigid star-shaped molecule in the different materials. Perspectives of this highly appealing molecule in the future researches will be also put forth.

1. Introduction

In recent years, polycyclic aromatic hydrocarbons (PAHs) that contain two or more closed aromatic ring structures have been actively researched due to their outstanding optoelectronic properties. To be well-characterized and usable, highly soluble structures have been developed, notably with the truxene core. Truxene (10,15-dihydro-*5H*-diindeno[1,2-*a*;1',2'-*c*]fluorene) is a planar heptacyclic polyarene structure obtained by trimerization of indan-1-one that can be considered as three annulated fluorene moieties. It can also be formally regarded as a 1,3,5-triphenylbenzene derivative with three -CH_2- "clips" added to rigidify the structure and keep the four phenyl rings coplanar. This polyarene exists under the form of two possible isomers, i.e. truxene **1** and isotruxene **2**, only differing in the way the fluorene moieties arrange (see Figure 1). The first reports mentioning the synthesis of "truxene" were reported in 1894[1,3] and 1942.[2] In the pioneer work of 1894, 3-phenyl-propionic acid cyclized in situ to indan-1-one under acidic conditions and subsequently self-condensed to give a mixture of truxene **1** and isotruxene **2**. A procedure yielding specifically the asymmetric isotruxene **2** was reported in 1960.[4] Concerning **1**, its selective synthesis was realized in early 1984 by Hartke and Schilling-Pindur starting from (3-methylthio)indene[5] and by Bergman and Egestad in 1986 starting from indan-1-one.[6] If the selective preparation of each isomeric form is now well-established, the symmetric form[7] has still received much attention than the asymmetric one and this review will only focus on this latter. To optimize the synthesis of truxene, synthetic approaches were diversified and tetrachlorosilane was proposed as an alternative to the strongly acidic conditions. However, reaction yield remained low, around 22%.[7] Reduction of truxenone **3** to truxene **1** by a variation of the Huang-Minlon Wolff–Kishner reduction was more successful and yielded **1** in 85% yield.[8] As specificity, PAHs **1** and **2** are characterized by a complete insolubility in common organic solvents. To overcome this drawback, introduction of solubilizing chains was studied and the first work in this field was reported in 1999 by Echavarren and coworkers who introduced three alkyl chains at the 2,7,12-positions.[9] In 2003, the first hexa-alkylated and highly soluble truxene derivatives were finally obtained, considerably widening the scope of application for this structure.[10] Notably, truxene derivatives received attention as starting materials for the construction of large polyarenes and structures analogue to fullerenes.[11,12] The first part of this review will thus discuss of the recent advances obtained in the chemical engineering of truxene and the development of new polyarenes.

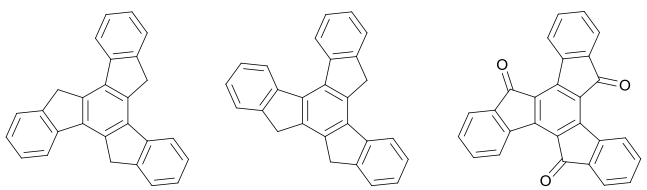

Figure 1. Structure of truxene **1**, isotruxene **2** and truxenone **3**.

Parallel to these studies only devoted to synthesis, the number of applications in which the truxene structure is involved has literally exploded, benefiting from the major breakthrough obtained in the peripheral functionalization of truxene. An immense variety of derivatives has been developed, where only the imagination is restrictive. At least twelve topics related to truxenes have been identified : non-linear opticals (NLO), two-photon absorption (TPA), transistors, organic photovoltaïcs (OPVs), organic light-emitting diodes (OLEDs), molecular resists, lasers, organogels, fluorescent probes, self-assembly, molecular wires, liquid crystals and dynamic nuclear

polarisation. The second part of this review aims at pointing out the added-value brought by the presence of truxene moiety in these different research fields.

2. Chemical Engineering around the truxene Scaffold.

Truxene is a fluorescent polyaromatic structure that exhibits a poor solubility in most of the common organic solvents in its unsubstituted form. To address this issue, introduction of solubilizing groups on the peripheral aromatic rings or functionnalization of the internal bridging -CH_2- groups was examined.

2.1. The truxene scaffold.

As above-mentioned, the first trialkylation of truxene was reported in 1999 by Echavarren and coworkers.[9] Depending of the reaction conditions, a mixture of *anti* and *syn*-derivatives was obtained. Thus, generation of the trianion at the 2,7,12-positions with KH or *n*-BuLi furnished a mixture of *anti* and *syn* trialkylated truxene **4** and **5** in 3:1 to 1:1 ratios, whereas use of sodium[13] or NaH provided exclusively the *anti*-derivative **4**. However, formation of **4** is not definitive and **4** can be easily isomerized to the more stable *syn* isomer **5** by a base-catalysed reaction (using notably potassium *tert*-butoxide *t*-BuOK) (see Scheme 1).[14] Among all the substituents that have been examined, isomerization reaction only failed with 9-anthracenyl as a result of the specific steric hindrance generated by this group.[15]

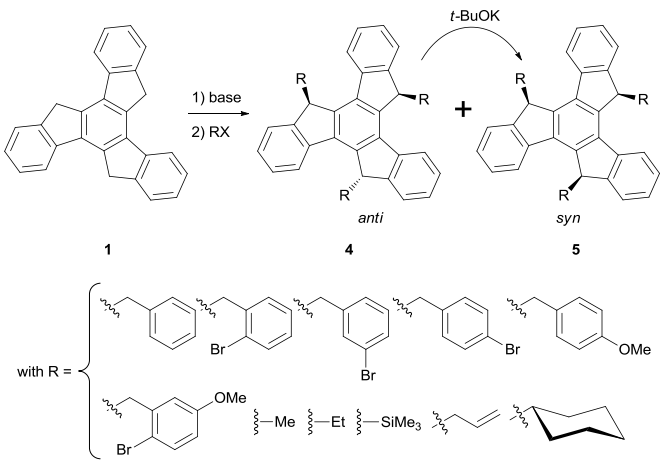

Scheme 1. Alkylation of **1** and conversion of the *anti*-derivative **4** to the more stable *syn*-derivative **5**.

2.2. Towards cage structures and bowl-shaped fragments of fullerenes.

The aforementioned tri-functionalization of the bridging -CH_2- groups was notably used to prepare polyarenic structures more extended than truxene and even cage structures. To illustrate this, truxenephane **6**[9] was obtained by reaction of the truxene trianion with tribenzyl bromide whereas the bowl-shaped fragment of fullerene **7** was synthesized in two steps by reaction with 2-bromobenzyl bromide followed by a subsequent palladium-catalyzed intramolecular arylation reaction of **8** (see Scheme 2). Using the same protocol, molecules **9-12** that exhibit a higher polyaromaticity than **8** were even prepared. However, the high insolubility of the reactional intermediates required an optimisation of the experimental conditions for the synthesis of each of these molecules.[16,17]

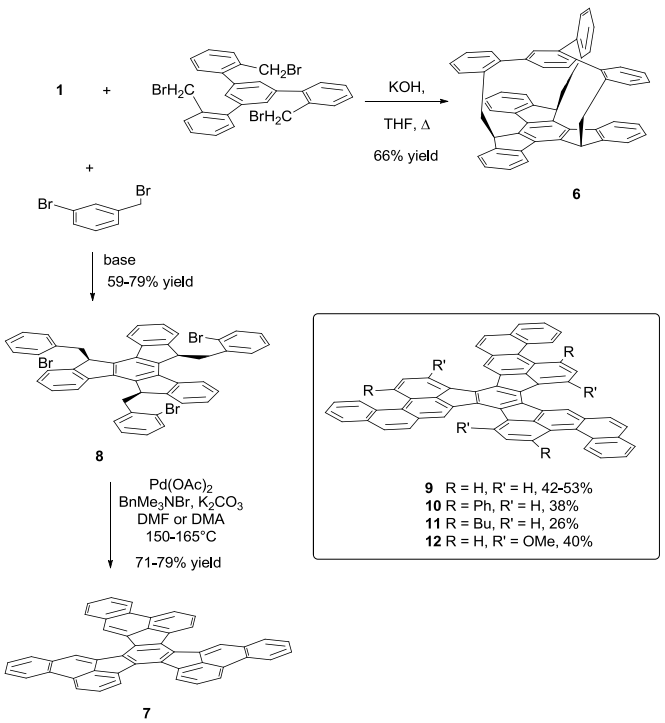

Scheme 2. Synthesis of truxenephane **6** and bowl-shaped fullerene fragments **8-12**.

Synthesis of these extended polyaromatic structures was not limited to the use of truxene as precursor but other structures were also prepared starting from the triaza analogue of **1**. As specificity, triazatruxene **13** comprises three carbazole units that share a common central benzene ring. To synthesize this molecule, two steps are required. In the first one, reaction of indole with Br_2 furnishes the symmetrical hexabromotriindole **14** in 18% yield.[18] In the second step, reductive debromination of **14** with triethylammonium formate and Pd/C yields **13** in 95% yield.[19] As previously observed for **8-12**, the synthesis of the extended polyaromatic structures **17** and **18** is obtained in two steps. Hence, *N*-alkylation of **13** followed by a palladium-catalyzed intramolecular arylation converted respectively **15** and **16** to **17** and **18**, providing nitrogen-based analogues of **8-12** (see Scheme 3). First investigations on the internal hexa-substitution of **1** were reported in 2005 and various aryl groups were used (see Figure 2).[20] As specificity, the selective synthesis of symmetrically or asymmetrically hexasubstituted truxenes could be achieved, by mean of the number of equivalents of base used during the reaction. Thus, use of 6 equivalents of *t*-BuOK gave the hexasubstituted truxenes **19-27** with yields ranging from 34 (for **26**) to 94% yield (for **24**).

Interestingly, the same reaction performed with a stronger base (n-butyl lithium (*n*-BuLi)) furnished lower reaction yields. Concerning the asymmetrically substituted truxenes **28**, **29**, the *anti*-isomer **29** was still obtained as the main product of the reaction, whatever the alkylating agent was, in a *syn/anti* ratio close to the theoretical 2:1 *syn/anti* ratio.

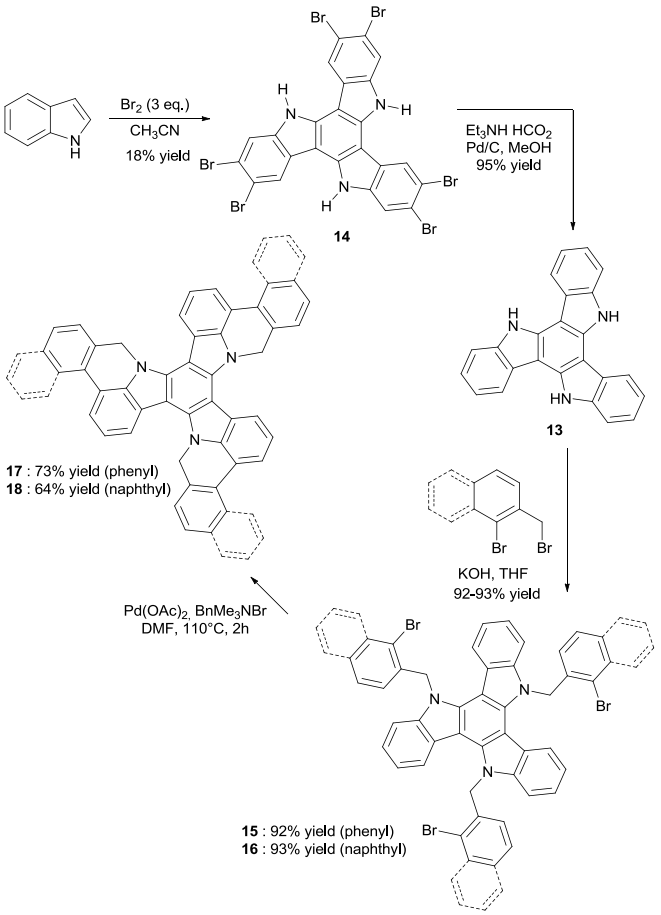

Scheme 3. Synthesis of triazatruxene derivatives **14-16**.

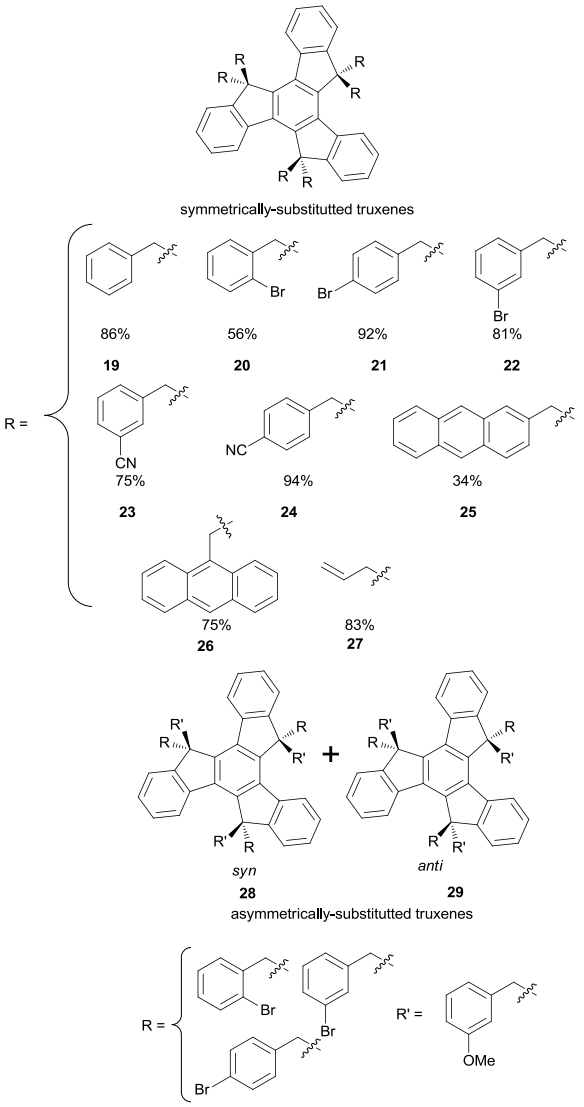

Figure 2. First examples of symmetrically and asymmetrically substituted truxenes reported in 2005.

Halogenation of truxene is another major issue as it opens the way to numerous ulterior functionalizations. The first electrophilic bromination of **1** was realized in 1894. In 2001, this reaction was revisited and a bromination yield as high as 92% was obtained for **30**.[21] Noticeably, post-functionalization of truxene proved to be a more effective strategy than the pre-functionalization of indan-1-one with halogens. If iodine is often preferred as substituent due to its higher reactivity in metal-catalyzed cross-coupling reactions, iodination of truxene with $[Ipy_2]BF_4$ furnished a mixture of diiodo and triiodo-compounds **31** and **32** that could not be further separated (see scheme 4). The selective preparation of the triiodotruxene **32** was realised in 2005 by the electrophilic iodination of **1** using H_5IO_6 and I_2 in acidic conditions, furnishing **32** in 90% yield.[12] From this moment, metal-catalyzed cross-coupling reactions (Stille, Suzuki coupling) of **1** became possible,[20,22] enabling to truxene to be used in a wide range of applications.

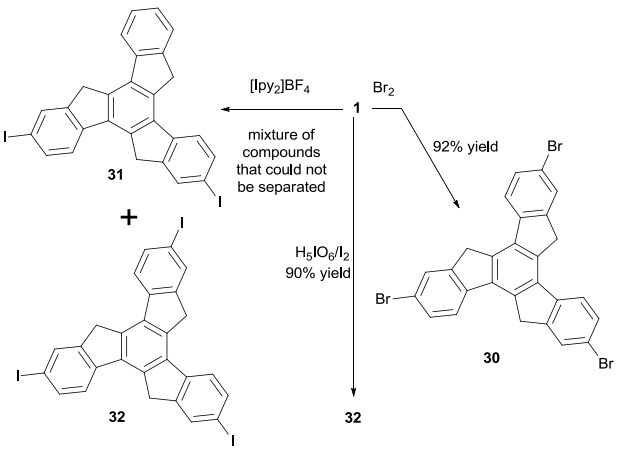

Scheme 4. Strategies developed for the tri-iodination of truxene **1**.

2.3. Towards polyarenes of high molecular weight.

As previously mentioned, the truxene scaffold has been considered as a potential building block for the design of various fragments of fullerenes and bowl-shaped structures. Several attempts were carried out to convert these bowl-shaped fragments to C_{60} and related carbon cages. The premise of this research was given in 1995 with the synthesis of the semi-Buckminster fullerene $C_{30}H_{12}$ also called "Buckybowl" **33**.[23] Cyclization of this structure was achieved by flash vacuum pyrolysis (FVP) at high temperature (1000°C) starting from the partially dehalogenated intermediate **34** (see Scheme 5). However, the synthesis of this molecule proved to be more difficult than anticipated and **33** was only obtained in 5-10% yield starting from **34** whereas the FVP of **35** only furnished traces of **33**. Low reaction yields were notably assigned to the difficulty to form simultaneously three five-membered rings. With aim at converting a bowl-shaped structure to C_{60}, the polyarene **36** that comprises the 60 carbon atoms of C_{60} but also 75 of the 90 carbon-carbon bonds of C_{60} has been synthesized in nine steps starting from **37** and subsequently converted to C_{60} by laser irradiation.[11] If the presence of the targeted molecule **38** was evidenced by mass-spectroscopy, no reaction yield was given for this reaction. This initial 9-steps route was replaced a year later by the same authors by a 12-step synthesis (starting from **40**) furnishing this times isolable quantities of C_{60}.[24] As specificity, the precursor **39** bears the chlorine atom at the key position and flash vacuum pyrolysis at 1100 °C formed the targeted C_{60} without forming any other fullerenes as by-products (see Scheme 5). However, the reaction yield remained extremely low, close to 0.1%. If the possibility to form C_{60} upon cyclization of **39** was thus brilliantly demonstrated, the viability of this approach for large scale synthesis of C_{60} has still to be demonstrated. Beyond the simple synthesis of fullerenes or fragments of fullerenes, elaboration of more sophisticated structures from truxene became possible thanks to the advances done in the introduction of peripheral substituents. In this field, star-shaped PAHs comprising hexa-*peri*-hexabenzocoronene can be cited as relevant examples.[12] Three PAHs **41**-**43** comprising respectively one, two and three hexa-*peri*-hexabenzocoronene units were synthesized starting from the highly soluble hexahexyltruxene **44** (see Scheme 6). In first step, **44** was iodinated using H_5IO_6 and I_2 under acidic conditions and the mono, *bis* and *tris*-iodinated truxene **45**-**47** could be selectively prepared. Then, the Sonogashira cross-coupling reaction with phenylacethylene furnished **48**-**50**. Finally, Diels-Alder reactions with tetraphenylcyclopentadienone followed by an oxidative cyclodehydrogenation of **51**-**53** with $FeCl_3$ furnished the three targeted PAHs **41**-**43**.

Using a similar strategy, perylenes were also fused to truxene (see Scheme 7).[25] To access to the perylenebisimide-based truxene **54**, two synthetic routes were developed in parallel, the first one being more straightforward and the second one being more versatile. As starting materials for the two synthetic pathways, two soluble perylenes **55** and **56** were prepared. In the two routes, the first step consisted in the Suzuki cross-coupling reaction of the perylene with **57**, giving **58** and **59**. The second step consisting in the photocyclization of **58** and **59** provided **54** and **60** in 95% yield. Finally, hydrolysis of **60** under acidic conditions followed by the amination of **61** with 3-pentanamine furnished **54** in 50% yield.

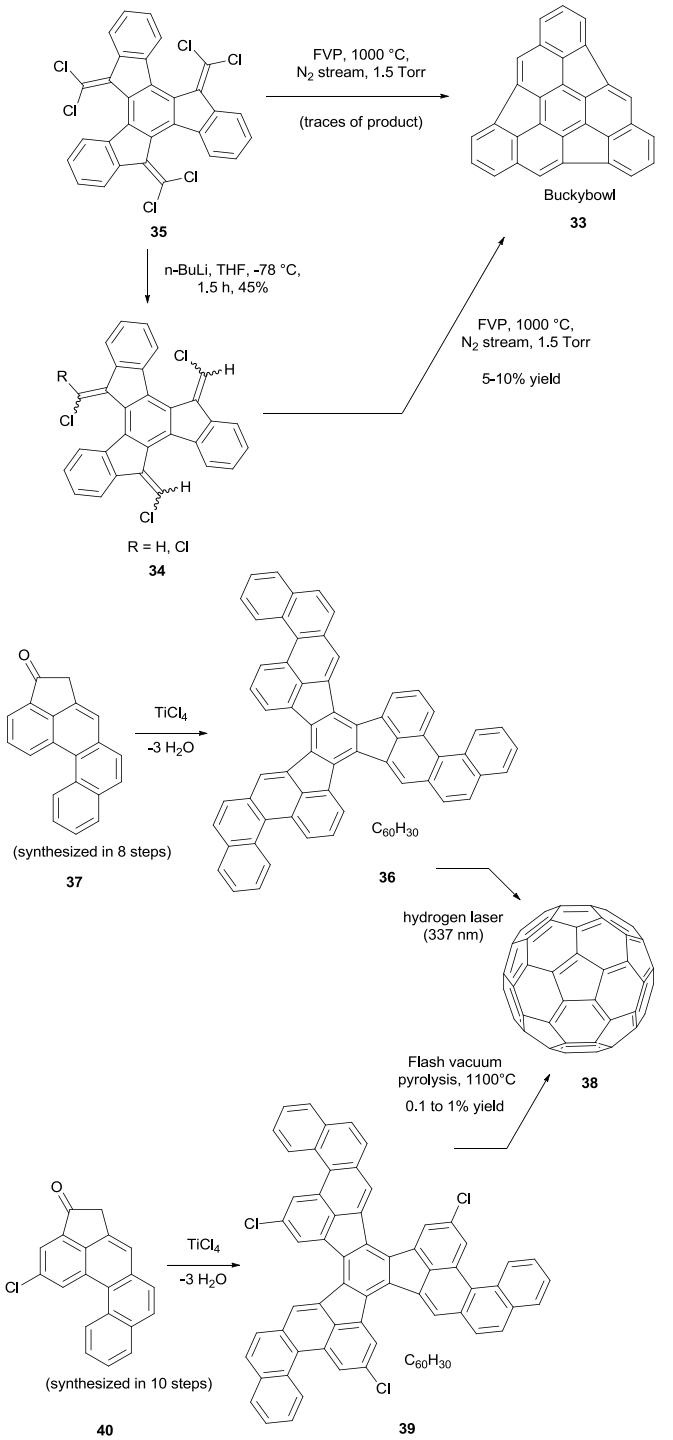

Scheme 5. Synthesis of bowl-shaped fragments of fullerenes **36** and **39**, precursors of C_{60} **38**.

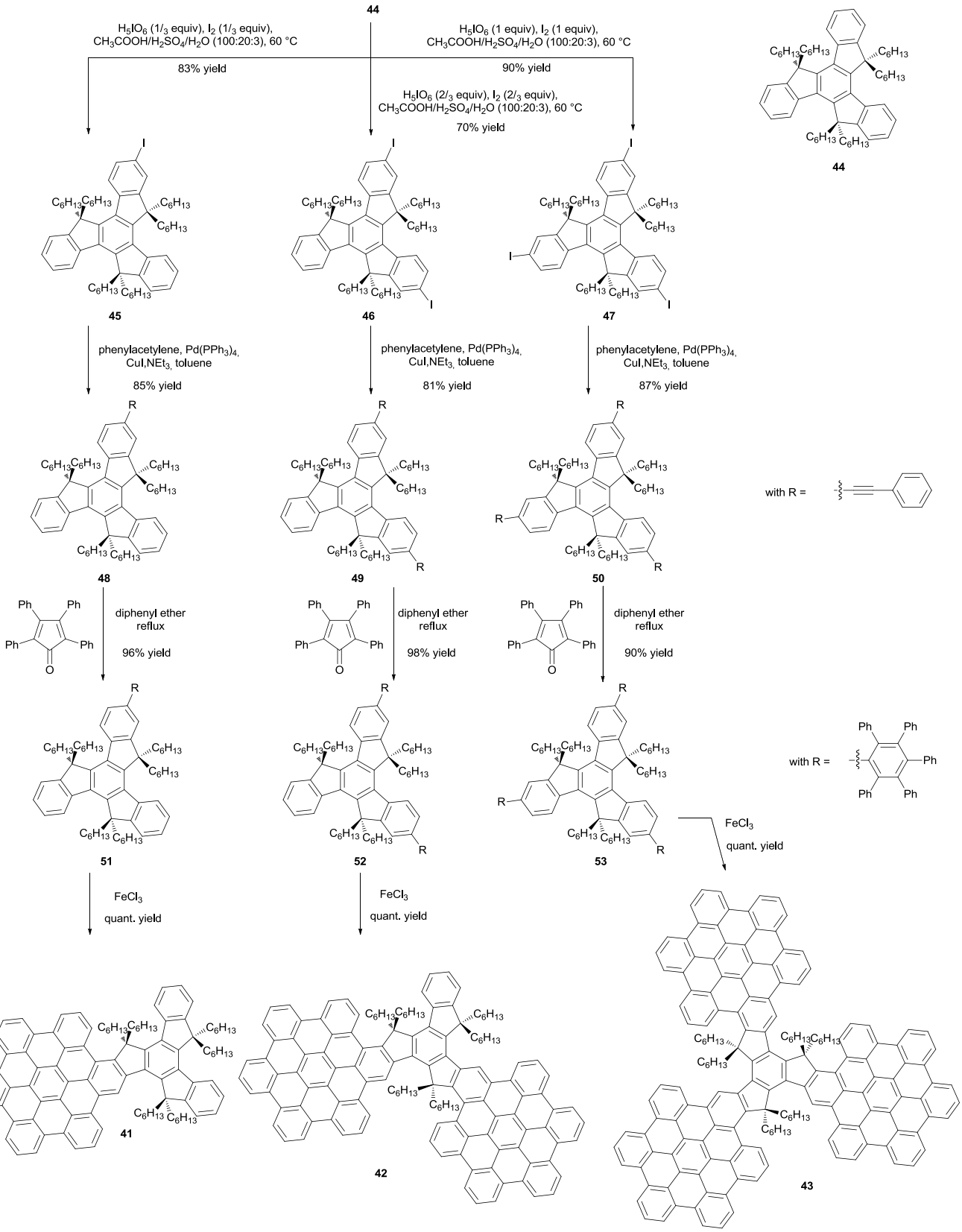

Scheme 6. Polycyclic aromatic hydrocarbons **41-4**3 containing peripheral hexa-peri-hexabenzocoronene units.

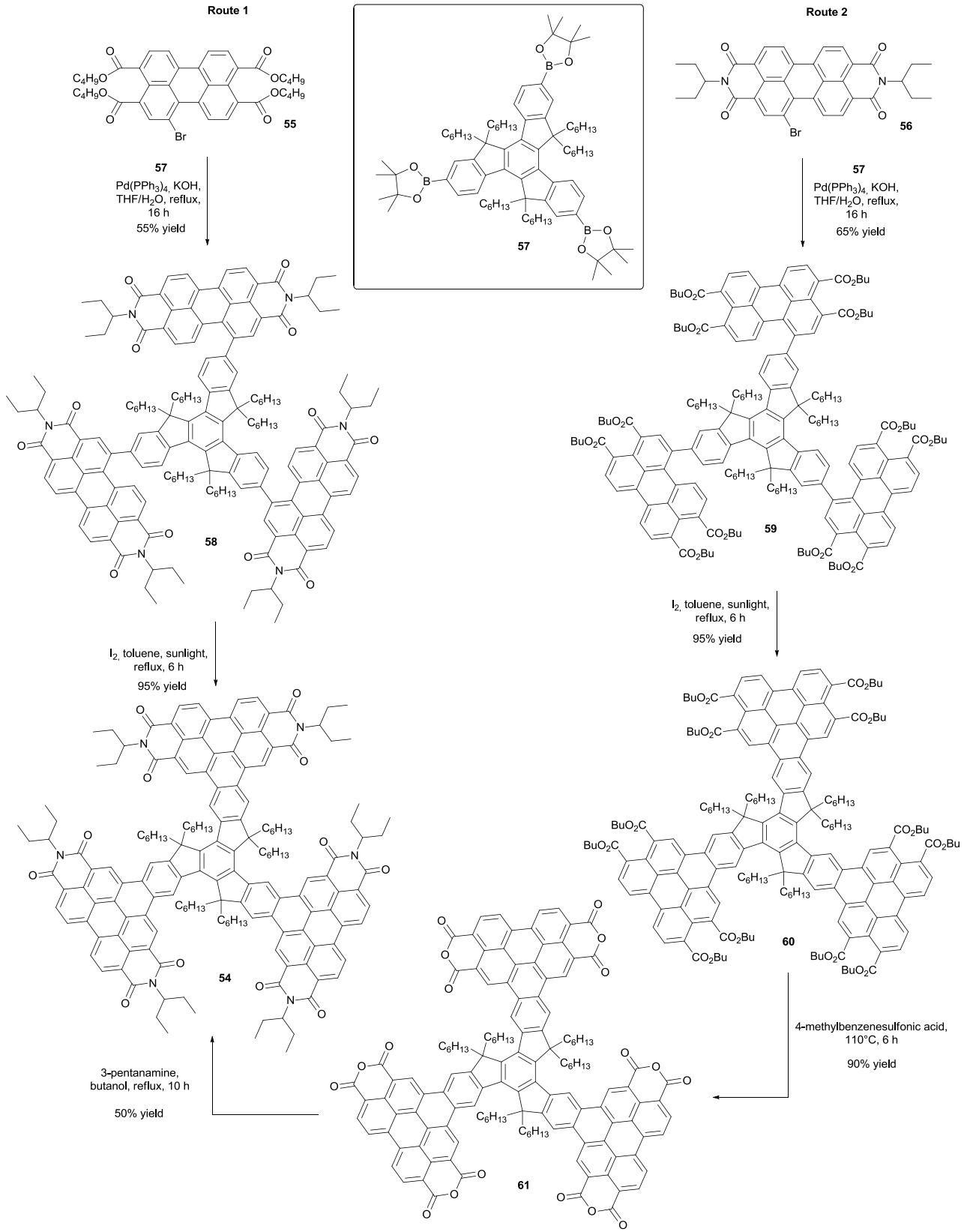

Scheme 7. Synthesis of extended polyarenes functionalized with peripheral perylenes.

Formation of molecular cages from truxene was not limited to single cage architecture. Double molecular cages sharing in common the same truxene platform were also prepared (see scheme 8).[26] Beyond the simple challenge of synthesizing double cages, authors also developed a new approach to access to the truxene core. Notably, truxene derivatives **62-64** were prepared in two steps, i.e. by double arylations of the triester **65** with various aryl lithium reagents followed by the acid-catalyzed intramolecular Friedel-Craft cyclization. Inspired by the synthesis of **6** and other cage-type structures,[27] double cage **66** was obtained by treating first **64** with BBr_3 followed by a double-capping reaction of **67** with tribromomesitylene. **66** was only obtained with the low yield of 10%. To end this part devoted to cages, triazatruxene **13** was also used as precursor for the formation of **68**.[28]

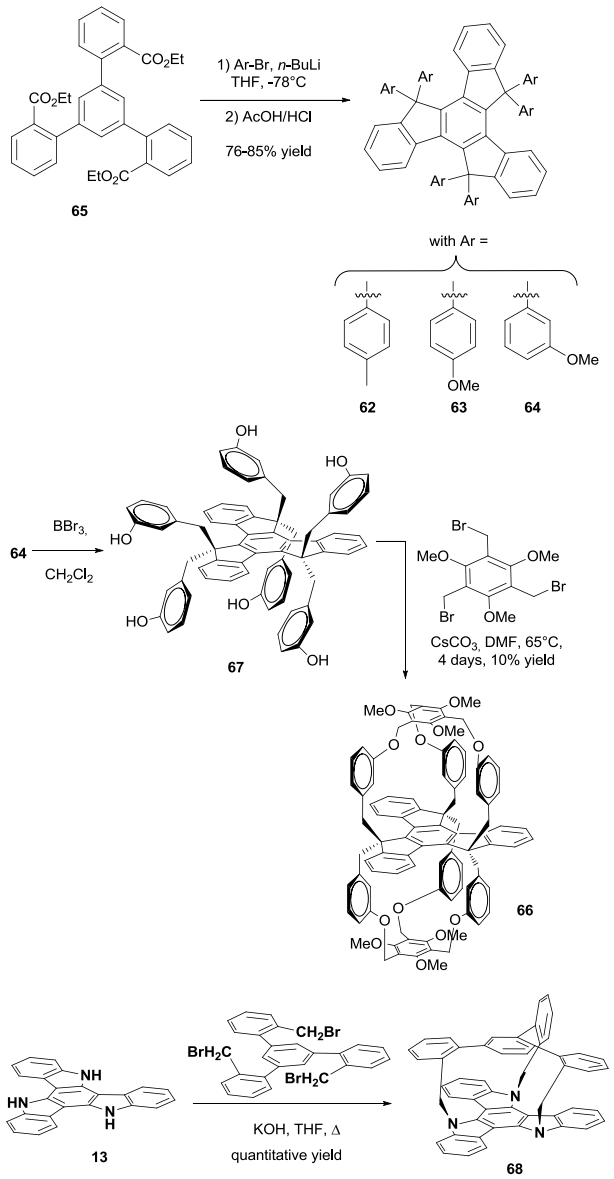

Scheme 8. Synthetic pathways to single and double cage molecule **66** and **68**.

In this last case, **68** was obtained in almost quantitative yield, contrarily to **6** that was obtained in only 66% yield (see Scheme 2). As observed for **6**, the central aromatic of the upper *tris*(benzyl)benzene in **68** is still forced into a cofacial arrangement.

3. Truxene derivatives and applications.

3.1. Dendrimers, oligomers and polymers.

Dendrimers have attracted a great deal of interest by their fascinating structures and their unique photophysical and mechanical properties.[29] First synthesis of truxene-based dendrimers was reported in 2003 and this paper constitutes a pioneer work in the design of π-conjugated dendrimers comprising polyarenes units.[30] To connect truxene units to each other, choice was done for a benzene ring that was formed by an acid-promoted cyclotrimerization of acetyl group in the presence of $SiCl_4$. Monacetylation of **44** was achieved by a Friedel and Craft reaction, furnishing **69** in 83% yield. Due to the steric hindrance of truxene, subsequent acid-promoted cyclotrimerization generating "in-situ" the central aromatic ring using $SiCl_4$ met several difficulties and reaction yield proved to be highly dependent of the amount of $SiCl_4$ used for the cyclization. Notably, use of 20 equivalents of $SiCl_4$ only furnished the generation 1 of the dendrimer in 23% yield whereas use of 30 equivalents yielded **70** in 91% yield (see Scheme 9). Generation 2 could be obtained with the satisfactory yield of 72%, what is remarkable considering the steric hindrance issued from the generation 1-precursor.

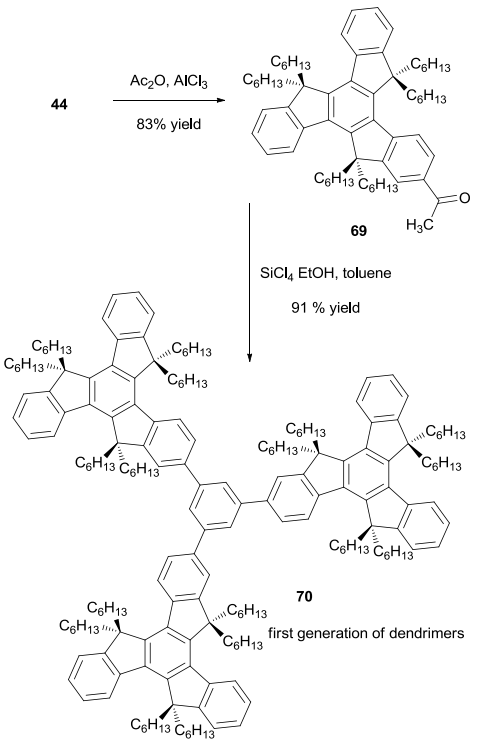

Scheme 9. **70**, generation 1 of dendrimers formed by cyclotrimerization.

From this initial report, numerous dendrimer-like structures were developed with rigid arms such as oligophenylenes,[31] oligothiophenes[10] and oligofluorenes,[32] or with conjugated arms such as triphenylamine dendrons.[33] Noticeably, all these studies were developed from the synthetic viewpoint and no applications were reported for these numerous dendrimers. Only the star-shaped molecule **71** was investigated in electroluminescent devices as a solution-processable emitter for the design of deep-blue OLEDs or as a host for various triplet emitters (see Figure 3).[34] Remarkable performances were achieved in the two cases.

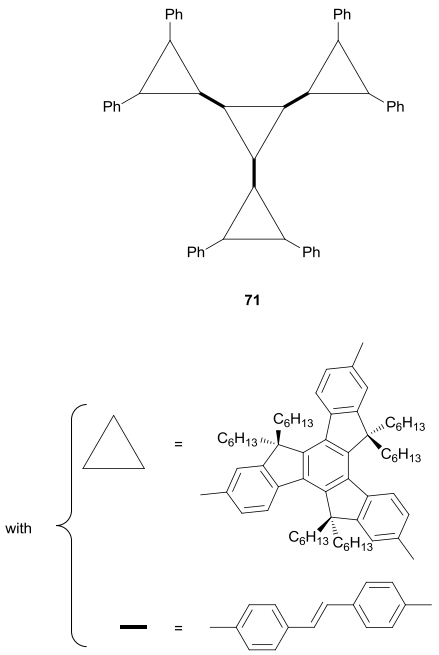

Figure 3. Structure of the star-shaped molecule **71**.

Recently, a great deal of interest has been devoted to develop dendrimers comprising metal complexes in their architectures. Notably, shape-persistent Ru-based macromolecules **72** and **73**[35] were presented as promising candidates for light-harvesting whereas the Ir-based dendrimers[36] **74** and **75** were reported as potential candidates for OLEDs. However, none of them were in turn tested in the mentioned applications. In the series of metal-containing dendrimers, only TruZnP **76** and TritruZnP **77** were synthesized for the examination of the photophysical properties of the resulting assemblies and finally examined for what was mentioned. Notably, mechanism of energy transfer existing between the two entities (porphyrin and truxene) was clearly established and elucidated (See Figure 4).[37] Finally, truxene-based polymers have attracted more attention than respective oligomers and dendrimers. Polymers were mostly developed to address the aggregation issue inherent to conjugated systems. Introduction of the truxene moieties into the backbone of polyfluorenes furnished hyperbranched and zigzag type copolymers **78-80** with a significantly reduced aggregation compared to that of the parent polyfluorenes prone to aggregation (see Scheme 10).[38] Indeed, one main drawback of polyfluorenes is to self-aggregate in the solid state, severely red-shifting their emissions relative to that observed in solution.[39] In the present case, no modification of the photoluminescence wavelength in solution and in the solid state was observed with **78-80** and a bright blue emission was obtained, evidencing that truxene can efficiently impede the aggregation formation. All polymers also exhibited an outstanding thermal stability as the onset degradation temperature was higher than 400°C. However these values are similar to that observed for polyfluorenes, suggesting that the incorporation of the truxene moiety does not affect the thermal properties. Recently, hyperbranched ladder-type poly(*p*-phenylene)s **81-84** were synthesized (see Figure 5). Despite the three dimensional structures of these copolymers, the resulting materials were soluble in most of the common organic solvents and capable to form high quality amorphous films. Especially, their PL spectra showed only slight differences when changing from solution to films, evidencing the crucial role of truxene in preventing from aggregation. These polymers were prepared by a Suzuki cross-coupling reaction which is the most common coupling strategy for the synthesis of molecules containing the truxene unit. For a higher reactivity, the boronic function is often attached to the truxene moiety as exemplified with **85** used as reagent for the synthesis of **86** (See Figure 6).[40] However, other reactions can also be used to prepare hyperbranched copolymers and Click chemistry was proposed as a possible alternative to metal-catalyzed cross-coupling reactions.[41] If the resulting polymers **87-90** exhibited a good thermal stability (onset degradation temperatures above 330°C), hyperbranched structures still showed a strong aggregation in the solid state with a blue emission in solution red-shifting to yellow in the solid state.

3.2. Photoresists.

In the previous paragraph, all polymers were prepared classically, by thermal polymerization of monomers. But polymers can also be photochemically generated. Recently, truxene derivatives were studied in this specific context of the photopolymers. Instead of being incorporating in the polymer backbone, truxene derivatives were used as photoinitiators of polymerization and these latter could be found after polymerization in the resulting crosslinked polymer network, blended with the polymer. Interest of using truxene in the design of new photoinitiators was first to greatly enhance the reactivity of the photoinitiator by increasing its molar extinction coefficient while shifting its absorption to the visible region and thus to provide a better adequation between the emission spectrum of the irradiation lamp and the absorption spectrum of the photosensitizers. In this recent and emerging research field in which we strongly contribute,[42a] truxene was notably functionalized with benchmark photoinitiators such as benzophenone (**91**) and thioxanthone (**92**),[42b] 2,2′-dimethoxy-2-phenylacetophenone (**93**),[43] acridine-1,8-diones[44] (**94**,**95**) or pyrene[45] (**96**) (see Figure 7). Proof of the concept was clearly established with a higher reactivity enabling to decrease drastically the concentration of photoinitiators, a faster

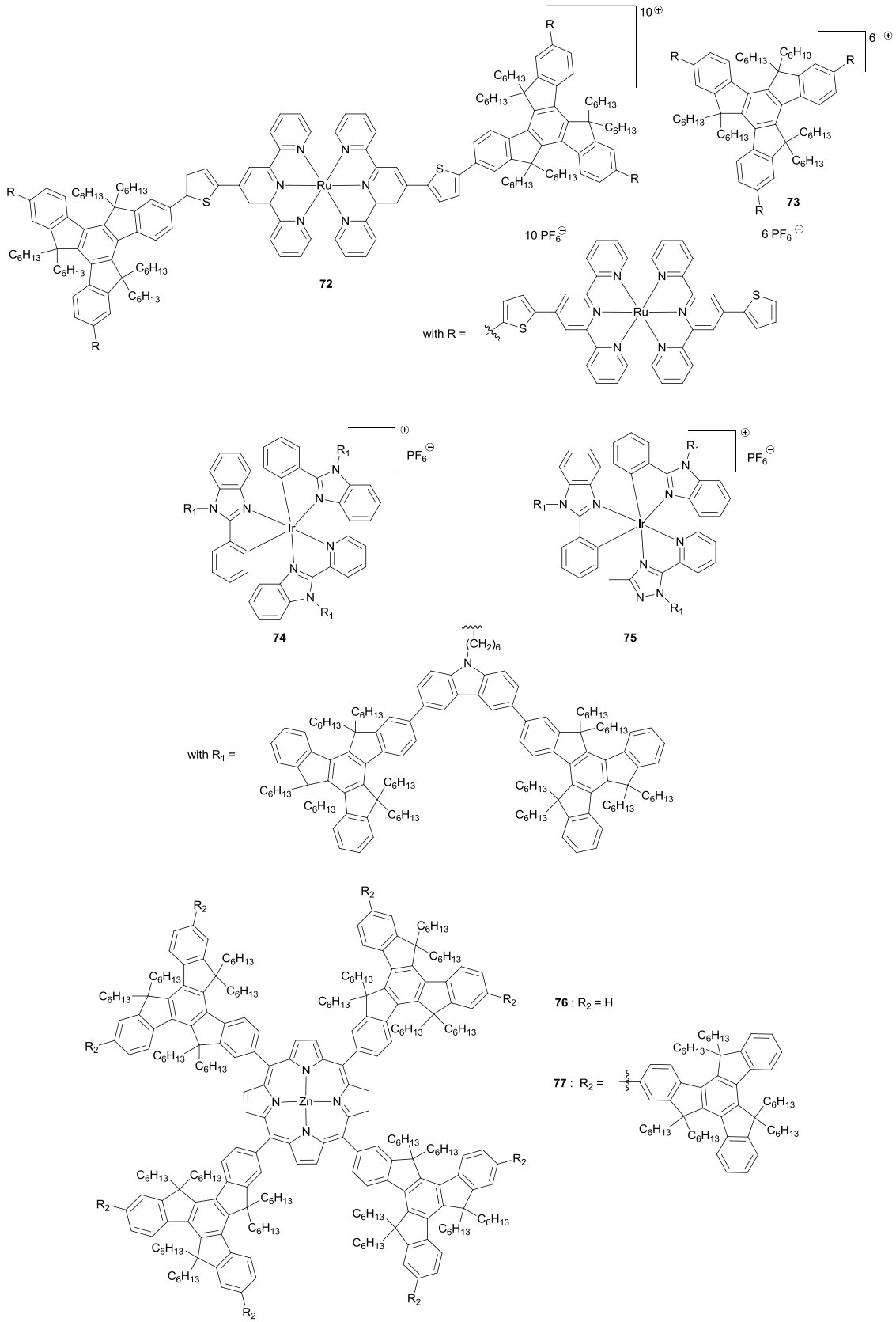

Figure 4. Ruthenium and iridium-based dendrimers **72-77**.

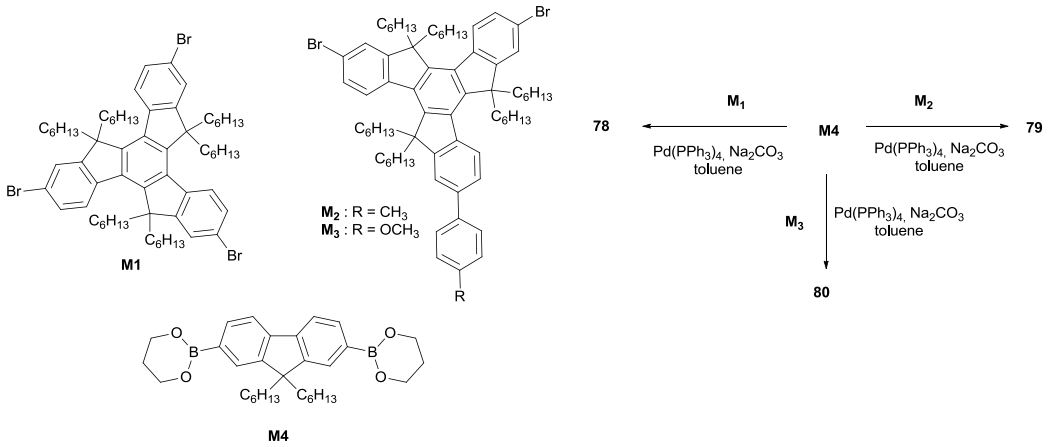

Scheme 10. Truxene-based conjugated polymers **78-80**.

polymerization compared to the benchmark photoinitiators and a higher degree of monomer conversion. In a completely different field, truxene was also incorporated in photoresists, without acting this time as photoinitiators. Photoresists **97** and **98** were notably used as semiconductors for photonics applications.[46] One critical issue of organic lasers is that the organic semiconductors often rapidly degrade in an none-controlled environment.[47] Notably, origin of this rapid degradation is mostly due to heat engendered upon laser operation and inducing a thermal decomposition of the materials. To isolate the organic semiconductor from its environment and to create an oxygen barrier, one way consists in embedding the semiconductor in an appropriate polymeric host matrix. Notably, star-shaped polymers are excellent candidates by their high thermal stability and low sensitivity to oxidation.[48] Truxene, by the presence of its six alkyl chains at the inner-position coming out of the plane, can also efficiently suppress its own aggregation when embedded in the polymer matrix. Beneficing of these advantages, photoresists containing **97** and **98** showed both an amplification of the emitted light and a higher stability of the semiconductor (see Figure 7). These new composites were thus considered as promising candidates for the laser/amplifying technology. Notably, the spontaneous amplified emission (ASE) regime could be established with **97** for pump energy density above 390 μJ cm^{-2}. Finally, truxene-based photoresists (**99-102**) were also developed for nano-patterning using e-beam lithography.[49] Photoresists containing truxene-based dyes **99-102** were notably found to exhibit an improved resolution compared to benchmark molecules while maintaining a good line edge roughness line width roughness. Especially, these interesting properties were observed for all dyes.

3.3. Organic lasers

In the previous paragraph, photoresists comprising truxene-based semiconductors were studied for laser applications. If initial works on lasers were developed around photoresists, recent investigations in this field are all devoted to develop solution-processable nanocomposites for an obvious easiness of fabrication. Notably, gain and lasing behaviour of **97** was revisited by the same authors in two different configurations, namely, by incorporating **97** into a transparent polyimide matrix, or in neat films overcoated with a poly(vinylalcohol) layer to mitigate the oxydation issue.[50] In the two cases, **97** was found to exhibit a low ASE threshold. Solid-state distributed feedback lasers using these materials showed a low-threshold and very broad tuning. A low ASE threshold of 2.1kW/cm² at 439 nm was notably achieved. While extending this study to **98** i.e. a higher homologue of **97**, a significant reduction of the threshold was achieved since this value decreased to 270 W/cm² at the same wavelength (see Figure 7).[51] More recently, **97** was revisited for developing a semiconductor laser for refractive index.[52]

3.4. Photoluminescence

First investigations of the photoluminescence properties of truxene from the theoretical and experimental point of view were reported in 1960[53] and more recently in 1998.[54] Comparison of the phosphorescence spectra of truxene with those of its parent triphenylene at 77K notably showed a strong band at about 1600 cm^{-1} in the triphenylene spectra originating from a ν8 benzene vibration delocalized over the four benzenic rings. On the opposite, analysis of the vibronic structures of truxene clearly evidenced this vibrational mode to be only localized on the central benzenic ring. These theoretical investigations were later extended to more complicated structures i.e. **97-98** and **103-109** (see Figures 7 and 8).[55,56] Shape of the molecules and the arm lengths were determined as being none innocent on the photoluminescence properties, the transition energies and the transition dipole moments of **97-98, 108-109**[57] even if these results confirmed general trends previously established.[22] The present study constitutes however the most detailed investigation ever reported on the photophysical properties of truxene derivatives. Red-shift of both absorption and emission combined with an increase of the molar extinction coefficient with elongation of the arm lengths

was clearly observed for all-truxene derivatives. Notably, for an oligofluorene arm of given length,[58] its molar extinction coefficient was determined as being three times higher after covalent linkage to truxene. Similarly, photoluminescence quantum yield (PLQY) was determined as increasing with the arm lengths. Conversely, radiative lifetime decreased with elongating the oligofluorene arms and the radiative lifetime was reduced for all oligomers grafted on truxene, relative to their parent oligomers.

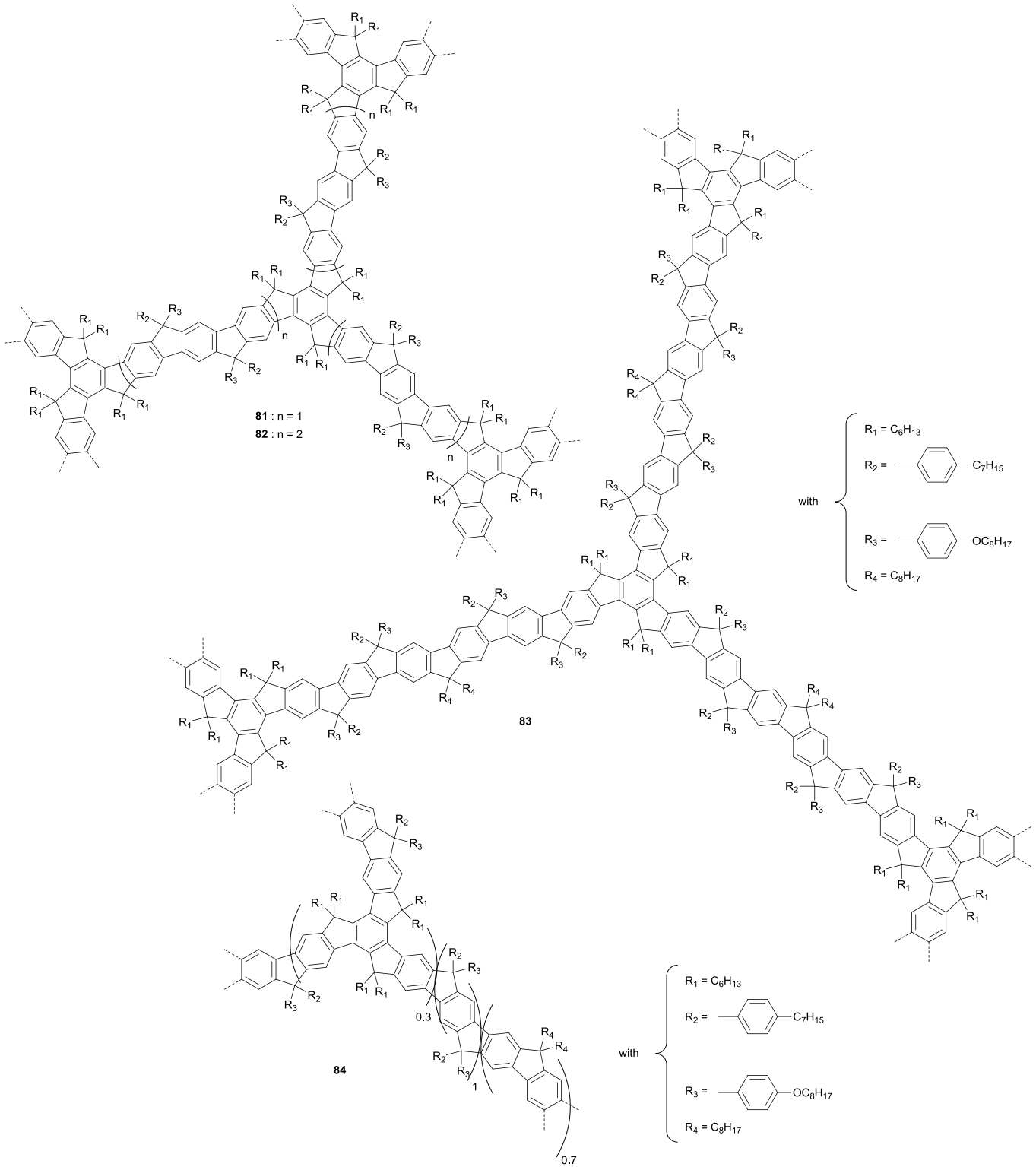

Figure 5. Hyperbranched polymers **81-84**.

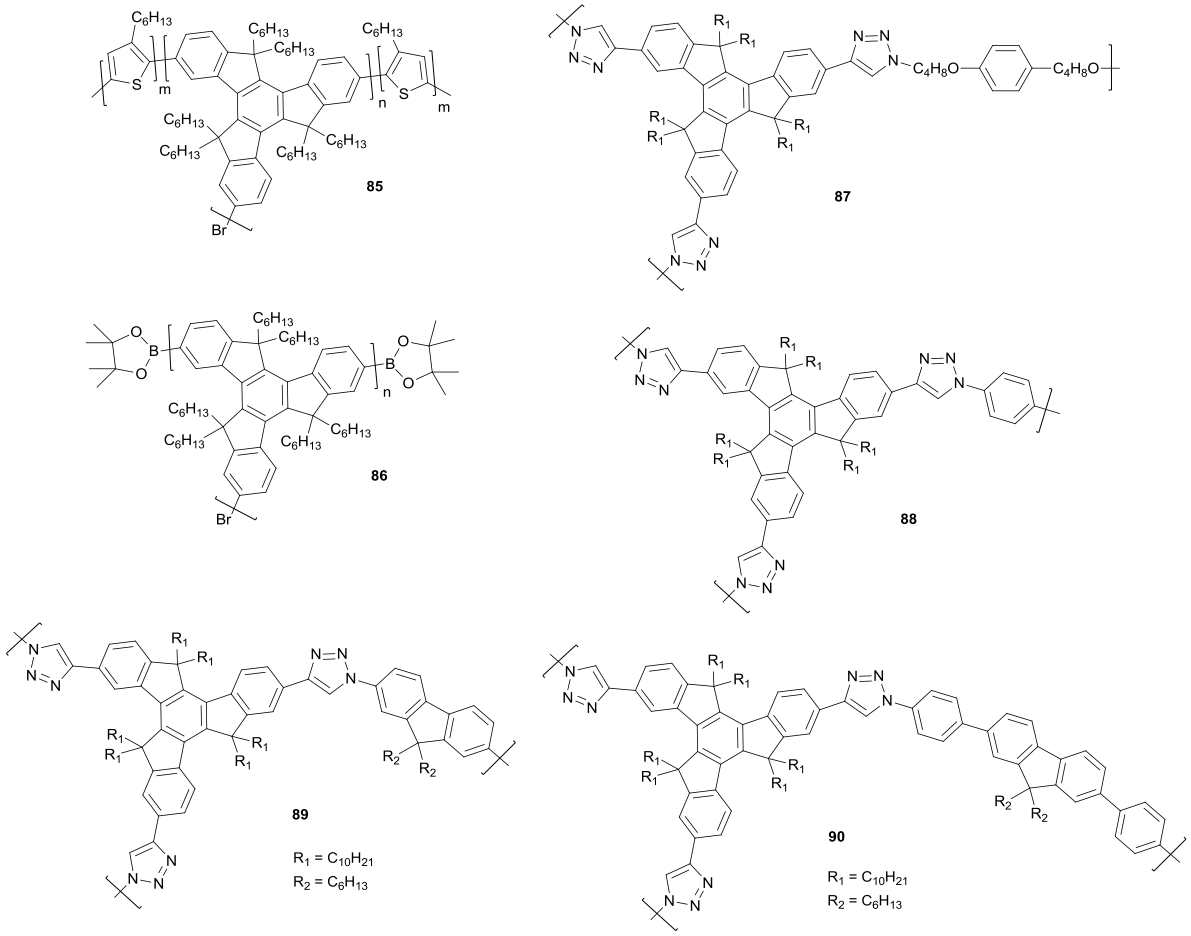

Figure 6. Hyperbranched polymers **85-90** prepared by Suzuki coupling or Click chemistry.

Concerning transition energies and dipole moments, these latter were determined as decreasing both in absorption and fluorescence with elongating the arm length. For these different systems, time-dependent density functional theory (TD-DFT) calculations also revealed the absorption to take place over the entire molecules, contrarily to the emission that is localized onto a single arm as a result of the C_3 symmetry of the molecules. Especially, **97-98** and **108-109** were proved to undergo a two-stage relaxation process.[59] To get a deeper insight into the photophysics of these molecules, influence of the location of an additional 2,1,3-benzothiadiazole unit in the arms of these molecules was examined. This study was realized with the series of molecules **110-114**.[60] In photoluminescence (PL), a pair-wise correspondence of the PL spectra of **110** and **113**, **111** and **112** was observed and rationalized on the basis of the molecular symmetry. The **111** and **112** pair showed the more red-shifted PL of the series. Conversely, the **110** and **113** pair exhibited a weak blue-shifted PL relative to that of **98**. However, if a variation of the emission wavelength was demonstrated, no influence on the PL lifetime or the PLQY was observed for all these molecules. Oligofluorene arms were also replaced by *p*-oliphenylene arms for photophysical investigations.[61] However, the general trends previously established were maintained. As anticipated, by increasing the effective conjugation length, emission maxima of the four compounds **115-118** were red-shifted from the ultraviolet to the blue region, showing that the emission wavelengths can be easily tuned with the length of the conjugated segments. As appealing feature, the stepwise increases of benzene rings also improved the thermal stability of these molecules and the glass transition temperatures (T_g) increased from 39°C for **115** to 192°C for **118**. Only a slight variation of the PLQY was observed, ranging from 0.91 for **115** to 0.93 for **116**, 0.98 for **117**, and 0.96 for **118**. Choice of the connection between the arms and the truxene core also strongly impacts the optical properties and this phenomenon was clearly demonstrated with the series **119-124**. Notably, use of double bonds as linkers was determined as facilitating the charge transfer compared to triple bonds (see Figure 8).[62] A similar trend was demonstrated with the series of ferrocene-substituted truxenes **125-128**.[63] Effectiveness of the electronic interaction between the ferrocene end-groups and the central truxene core could be finely tuned by mean of the different spacers and a red-shift of the charge transfer band with elongating the conjugated spacer was observed. As last structures investigated for their PL properties are dumbbell or twin molecules **129-136** bearing two

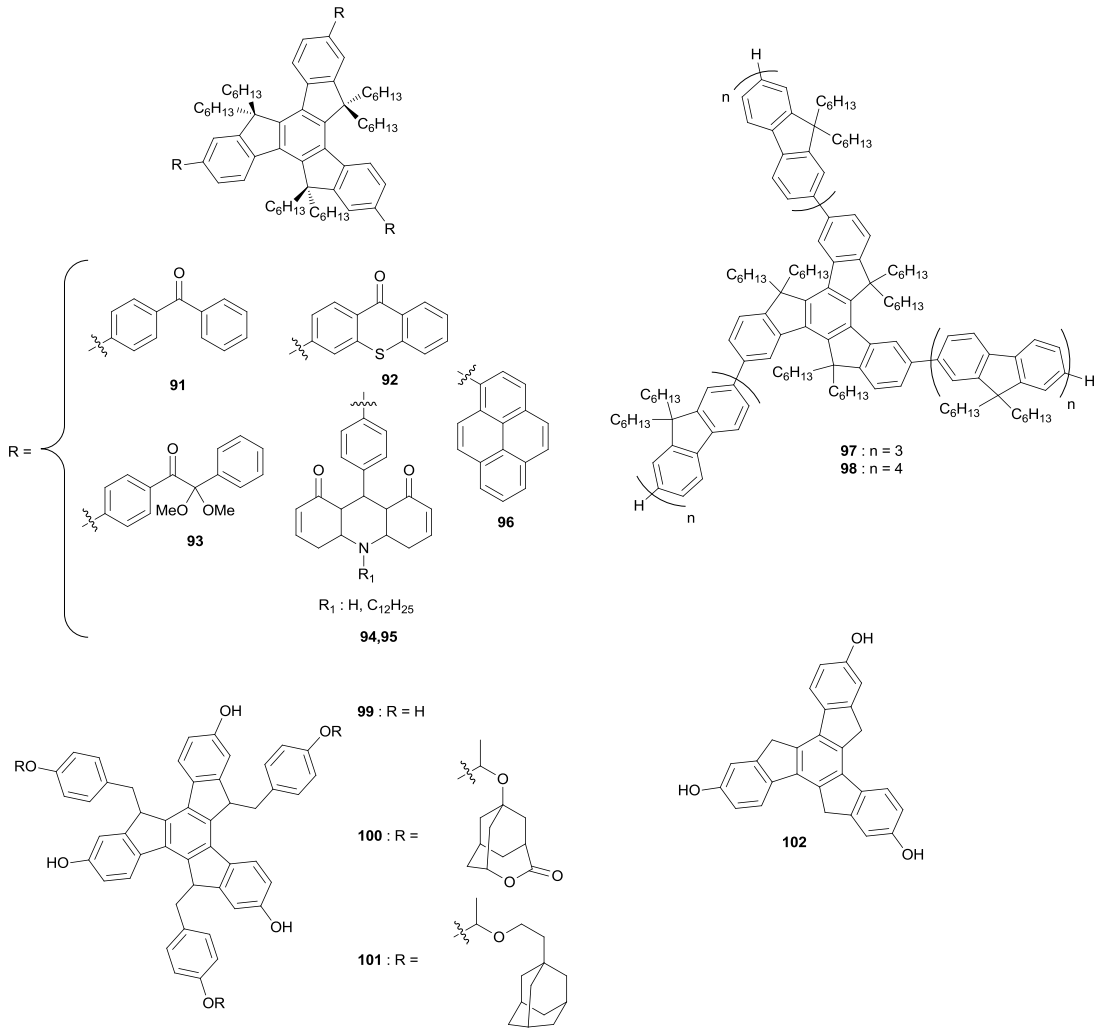

Figure 7. Truxene-based photoinitiators **91-98** and structures of truxene derivatives incorporated in photoresists and polymer blends (**99-102**).

truxenes halves connected by mean of a conjugated spacer (see Figure 8).[64] While using oligo(thienylethynylene) spacers, saturation of the effective conjugation length was achieved for **133** as its maximum emission wavelength only shifted of 2 nm compared to that of **132**. A clear decrease of the PLQYs with elongation of the rigid segment was observed, namely 0.25 for **129**, 0.22 for **130**, 0.20 for **131**, 0.20 for **132**, and 0.18 for **133**, resulting from molecular aggregation in the solid state. However, PLQY of **129-133** remained significantly higher than that of the oligo(thienylethynylene)s considered separately. Introduction of truxene units thus strongly limited aggregation of oligo(thienylethynylene) chains. To definitely prevent aggregation, a logical extension of this work consisted in introducing a bulky group in the bridge connecting the two truxene moieties, what was realized with **134**. 9,9'-Spirobifluorene bridge in **134** could efficiently suppress the intermolecular π-π aggregation in the solid state and only a limited red-shift of the PL maximum peaks both in solution and the solid state was observed (388 and 411 nm in solution versus 394 and 412 nm in the solid state respectively). On the opposite, a more pronounced red-shift from 408 to 431 nm was obtained for **136** due to its two-dimensional topology favorable to aggregation. Finally, all these investigations on the determinant role of the linkers on the electronic interactions, the crucial role of the length of the conjugated chains on the optical properties paved the way to the study of new structures highly sensitive to the length of the conjugated system and the electron-donating or releasing character of the end-groups, namely push-pull molecules. Numerous truxene-based push-pull chromophores were developed and contained porphyrins (**137-142**),[65] triphenylamines or dimesitylboryls (**143-150**) as electron-rich/deficient groups (see Figure 8).[66] As anticipated, elongation of the conjugation of the peripheral substituents in **137-142** red-shifted the absorption peak of the truxene moiety without affecting the position of the Q-bands specific of the porphyrin moiety. However, upon grafting of the truxene

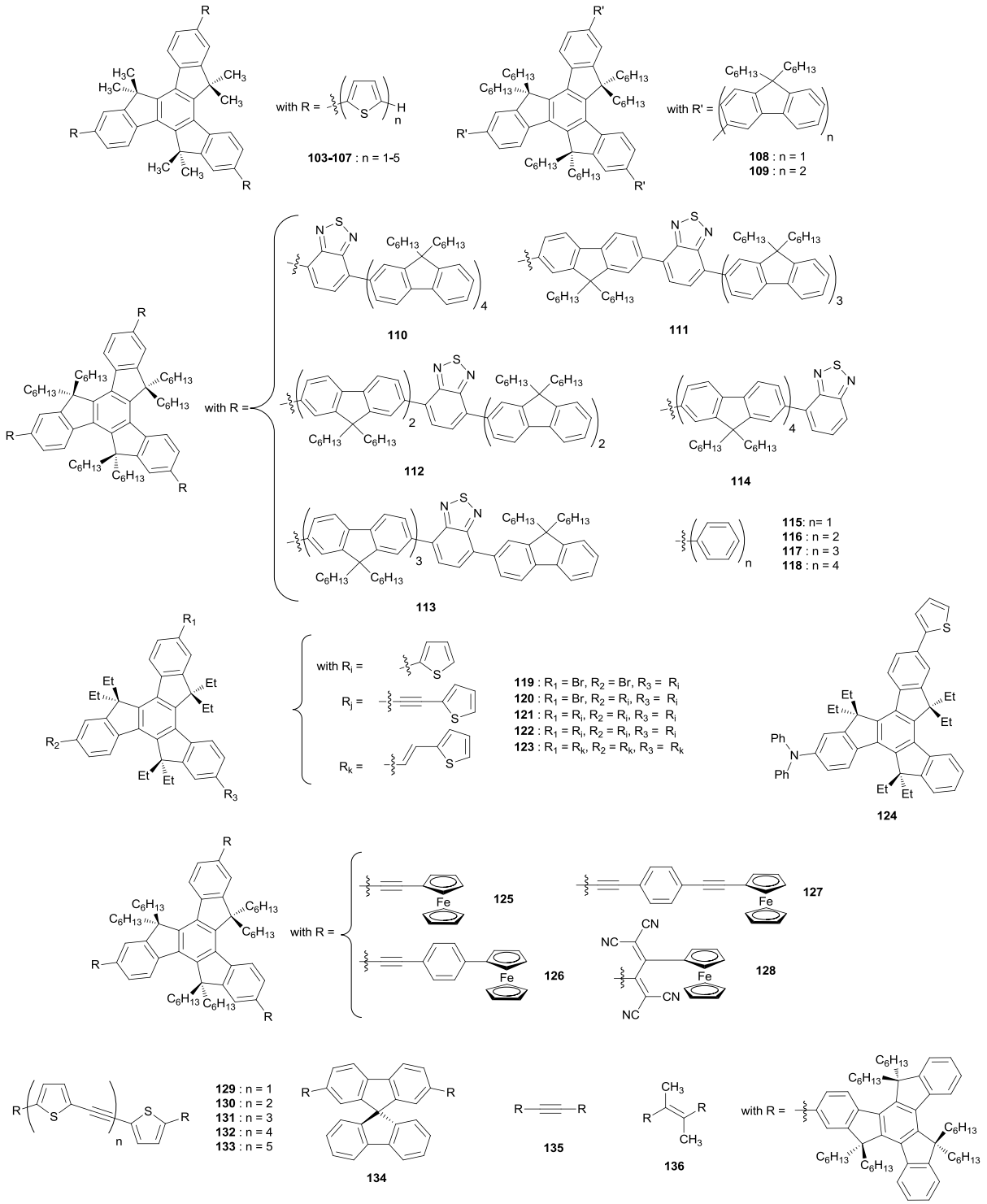

Figure 8. Truxene derivatives **103-118** prepared for photophysical studies, ferrocene-based truxenes **125-128** and Dumbbell molecules **129-136**.

moities, a significant enhancement of the PLQY was observed. It notably increased from 0.11 for the free porphyrin to 0.19-0.30 after functionalization. When connected to the electrodeficient three-coordinate organoborons or the electron-rich triphenylamine, the truxene core by its extended electronic system could indifferently act as the electron-releasing or the electron-withdrawing group. Here again, a major enhancement of the PLQY was achieved since it increased from 0.07 for

truxene to 0.27 for **148** and 0.34 for **145**, so about 4-5 times higher. Enhancement of the fluorescence of **145** and **148** was tentatively assigned to a photoinduced charge-transfer. One year later, a deeper insight in the solvatochromism of truxenes bearing terminal dimesitylboryl acceptors was carried out. A large and anomalous solvatochromism of their emission spectra was clearly evidenced.[67] Notably, emission spectra of these molecules proved to be highly sensitive to the protic or aprotic character of the solvent, whereas their absorption spectra remained unchanged. Thus, emission maxima of **149** and **150** shifted from 160 nm with the solvent polarity, from 420 nm in hexane to 580 nm in acetonitrile, making these molecules ideal candidates for polarity probing. The diverse and fascinating properties of push–pull chromophores inspired the synthesis of numerous molecules such as **151-152** which exhibited a conventional solvatochromic behavior[68] or structures in which the emission of truxene could not be detected anymore. This behavior was notably observed for multichromophoric systems in which truxene was covalently linked to dyes of high PLQY such as Bodipys (**153-160**)[69] or perylenes (**54**) (see structure in Scheme 7).[70] In these different cases, no residual emission of the truxene core could be detected whatever the excitation wavelength, evidencing the quantitative intramolecular energy transfer from the truxene core to the peripheral fragments. As a result, magnitude of the molar extinction coefficient of **54** was clearly far from the three folds of perylene bisimides (PBI)'s indicating that the three PBI groups in **54** are no longer independent chromophores but have integrated a larger π-conjugated system. From the PL viewpoint, electronic interactions between truxene and perylenes reduced the PLQY of **54** to only 40% that of the parent PBI.

Multichromophoric systems were also designed with metal complexes. With regard of fine tuning the electronic/energy transfer between complexes of bimetallic structures, truxene could advantageously switched the energy-transfer mechanism from Förster- to Dexter-type.[71] In **161** and **162**, truxene could promote an efficient energy transfer between the two metal centres without affecting the electronic properties of the individual components. Mechanism of the energy transfer between the two metal centres could even be decomposed. Upon photoexcitation, the first energy-transfer step from the truxene to the metal centres was determined as being based on a Förster mechanism. After an ultrafast intersystem crossing, the energy transfer for the ^{3}Ru→^{3}Os process was found to be much faster than that predicted for a Förster mechanism, suggesting the allowance of through-bond mediated Dexter mechanism. As a result, a slight reduction of the PLQY of these bimetallic architectures was observed. More generally, reduction of PLQY was observed for all polymetallic structures (**161-163**) (see Figure 10). On the opposite, PLQY of mononuclear complexes such as **164** and **165** that contains only one metal centre attached to truxene increased about 40% compared to the complexes without truxene.[72] Following this work, trimetallic systems comprising Os, Ru and Pt metal centres (**166**)[73] or hybrid organic–inorganic multichromophoric structures associating metal complexes and Bodipys (**167-169**)[74] were investigated. Here again, the role of truxene was not only to ensure the linkage between the peripheral groups but also to act as a photoactive component that enriches the photophysics of the assemblies. Notably, a severe reduction of the PLQY was observed for all multichromophoric arrays comprising Bodipys compared to the PLQY of the Bodipys considered separately. Jointly, a red-shift of the emission peaks of **167-169** compared to that of the parent **170** was also observed, resulting from a higher π-delocalization in these structures. Likewise, organometallic multiads **171-174** composed of a porphyrin surrounded by platinum complexes and truxenes enabled to demonstrate an interchromophoric cooperativity in S_1 and T_1 energy transfers (see Figure 11).[75] Energy transfer rates in these systems were significantly dependent upon the number of donors. Existence of electronic interactions in multichromophoric arrays was confirmed with the study of the polymer **175**.[76] Evidence of a singlet and triplet energy transfer from the truxene moiety to the porphyrin and another from the platinum complex to the porphyrin were provided.

In all the above-cited examples, the donor was directly connected to the acceptor via a conjugated spacer. But the donor can also interact with an acceptor in supramolecular architectures, what was achieved with the study of the complementary pair of **176** and **177**.[77] Thanks to the close match in term of size, shape and symmetry, **176** and **177** were capable to self-assemble to form 1D microstructures in various solvents. Evidence of a mutual interaction between **176** and **177** was brought by mixing of the two molecules in solution, resulting in the dramatic color change. As additional proof, Differential Scanning Calorimetry (DSC) traces of the 1D microstructure showed that the phase-transition peaks of the individual components were not detectable anymore, indicative of the emergence of a new mesostructure. A strong decrease of the melting point was also detected, furnishing in turn liquid crystals properties to the self-assembly.

3.5. Fluorescent probes

Recently, truxene has been revisited in the context of developing new fluorescent molecular sensors. Fluorescent probes are one of the cornerstones of real-time imaging of live cells and a powerful tool for the detection of molecular entities in live cells or the recognition of ions in aqueous solutions.[78,79] As first example of molecular probes developed with truxene, water-soluble sensors specifically designed for the detection of porphyrin-containing metalloproteins were prepared.[80] These two species, **178** and **179**, that only differs by the number of carboxylic groups, were characterized by their high sensitivity to metalloproteins and the simplicity in data collection (see Figure 12). Especially, these two molecules showed a remarkable sensitivity to cytochrome C and myoglobin and the two proteins could be detected at concentration lower than 2×10^{-5} M. In the same spirit, **97** was successfully used for the detection of biomolecules (see Figure 7).[81] Notably, the avidin protein could be detected at concentrations lower than 1 μg/mL. The selectivity of the truxene sensor for this protein was clearly evidenced by introducing in the medium Bovine Serum

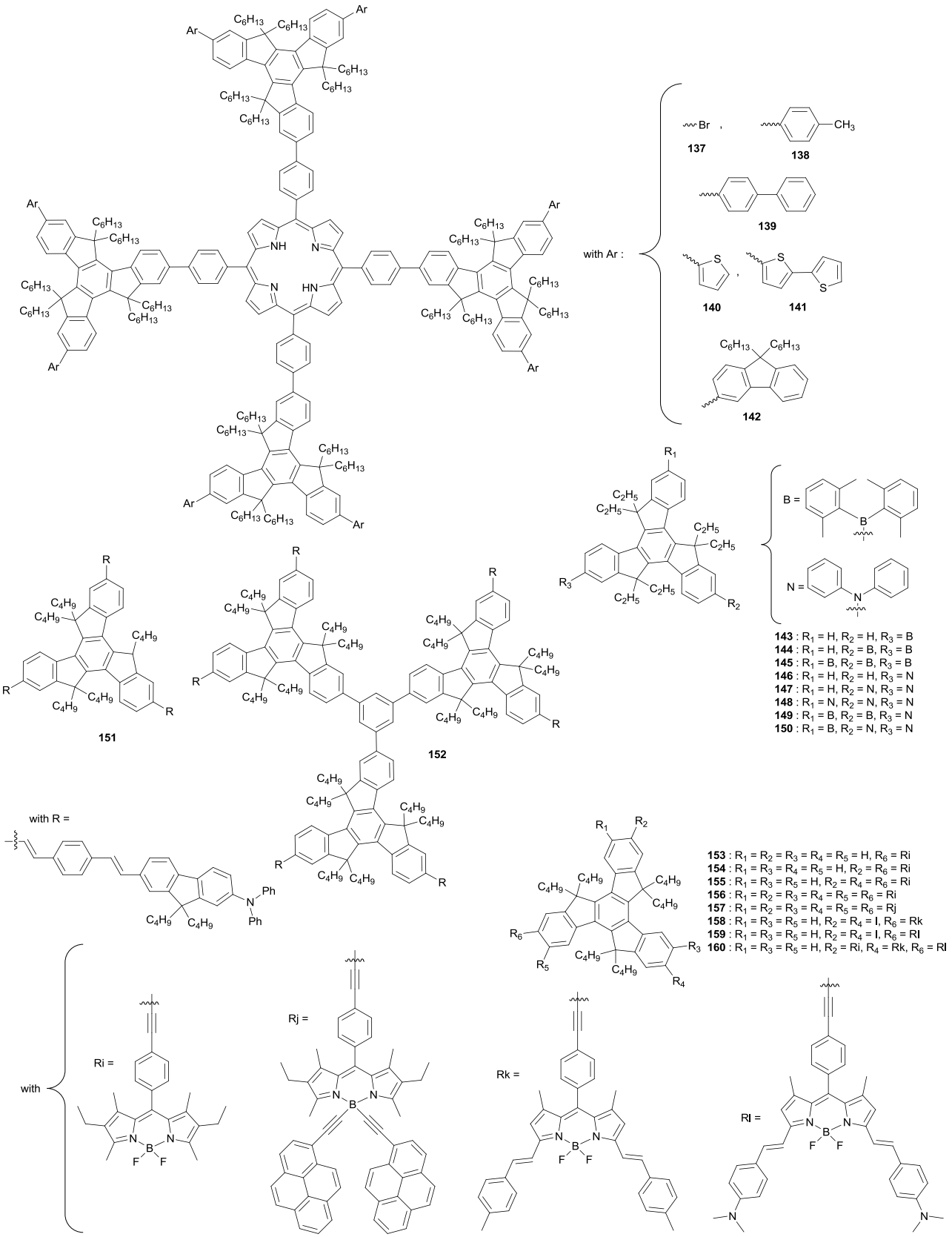

Figure 9. Push-pull chromophores **137-152** and Bodipy-based dyes **153-160**.

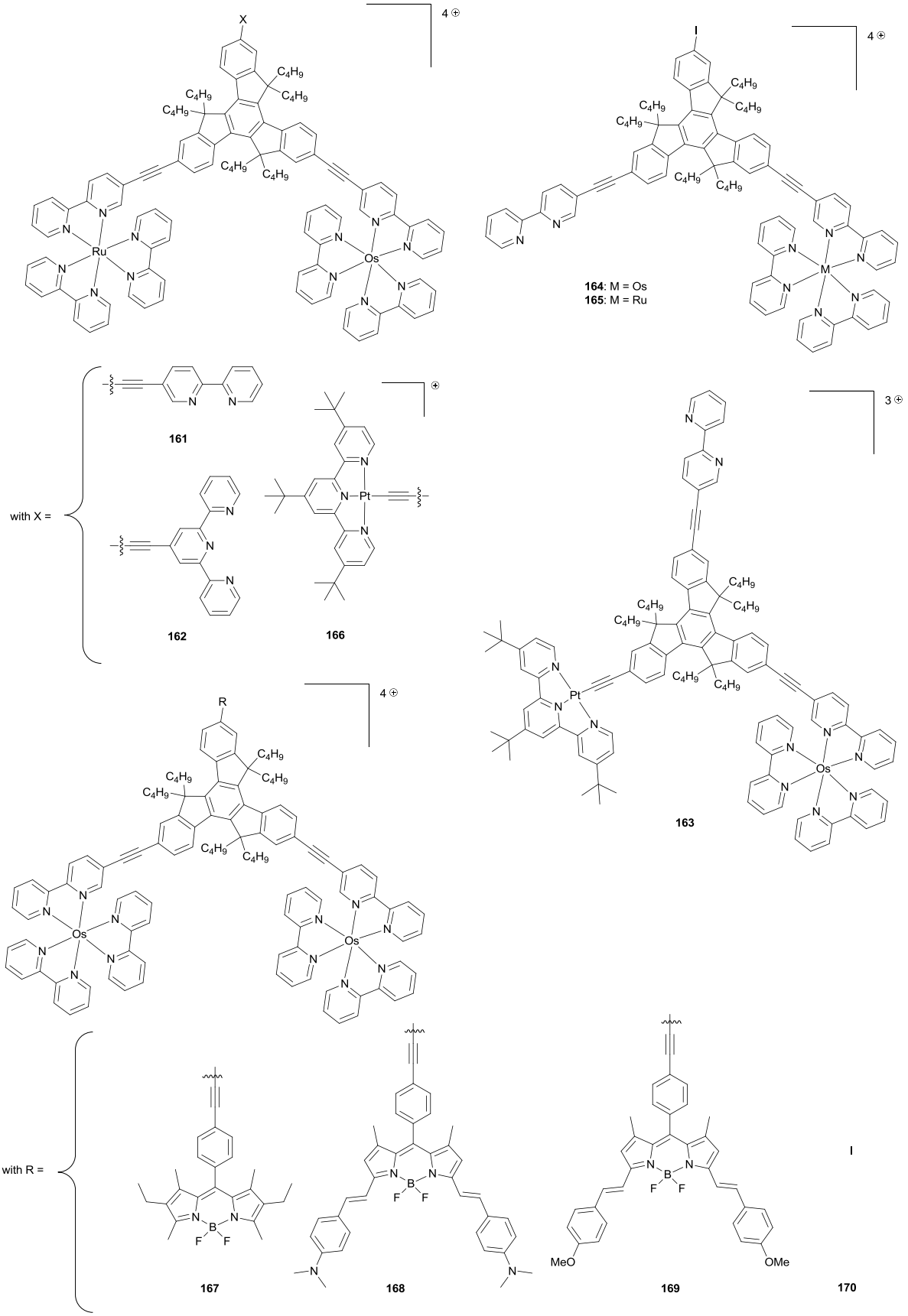

Figure 10. Structures of the multichromophoric arrays and organometallic multiads **161-170**.

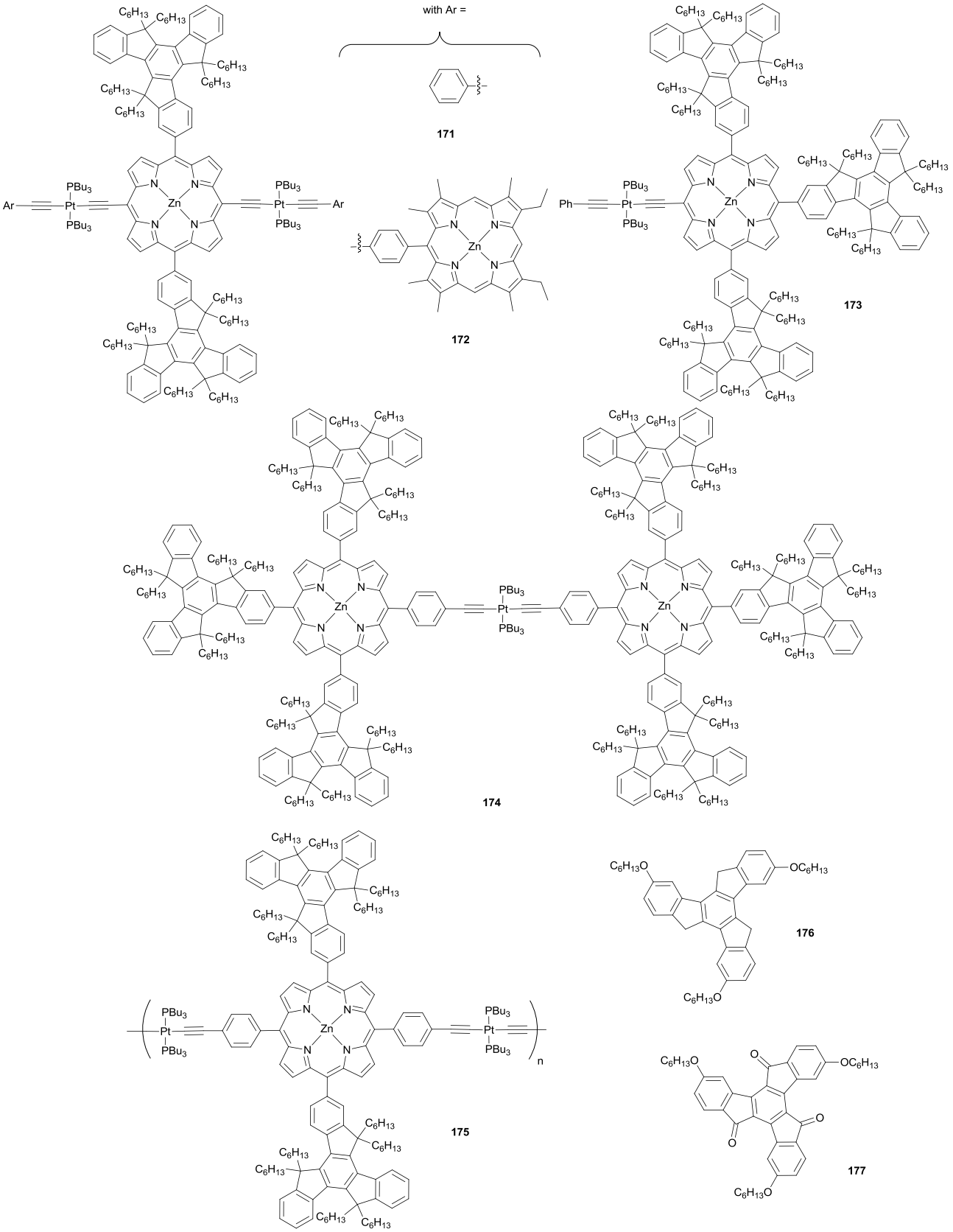

Figure 11. Porphyrin-based dyes **171-175** and the complementary pair **176-177** used to design 1D macrostructures.

Albumin up to 50 000 µg/mL without perturbating the detection of avidin. Truxene-based probes were also designed for the specific recognition of ions and, in this aim, the truxene-cored π-expanded triarylborane dyes **180** and **181** were synthesized.[82] Authors notably focused their interest on fluoride anions as these ions dramatically affect chemical, biological and environmental processes. The two probes were designed so that a completely different spectrophotometric response could be obtained with the two probes. In the case of **180**, a significant decrease of the PL intensity could be observed whereas the fluorescence of **181** was strongly enhanced in the presence of fluorides. Remarkably, a six-fold fluorescence enhancement was obtained. In the two probes, triarylborons were used as the selective binding sites for the analyte. The detection limits were low, ranging respectively from 12 µM to 13 µM for **180** and from 3 µM to 5 µM for **181.**

3.6. Organic Electronics

3.6.1. Organic Light-Emitting Diodes (OLEDs)

Since the pioneering works of Tang and Van Slyke on OLEDs, device elaboration has evolved towards multilayered devices with layers ensuring the different roles of charge injection and transport as well as emission.[83] When a triplet emitter is used, the emissive layer can't be composed exclusively of the phosphorescent emitter but this latter must be diluted in a material named host that ensures the isolation of the dopant molecules from each other.[84] Classically, the host is a hole-transport material (HTM), resulting in a strong imbalance of the charge transportation within the emissive layer. Thermal stability of the host is another crucial parameter as no phase transition or structural rearrangement of the emissive layer should occur during device operation. A high thermal stability of these materials is thus required. In this context, the trispirocyclic **182** met this criteria of thermal stability with a glass-transition temperature (T_g) higher than 170 °C.[85] When used as a HTM in a conventional multilayered device, ITO / HTM (60 nm) / Alq_3 (60 nm) / LiF (0.5 nm) / Al, device reached the maximum luminance of 37 000 cd/m² at 14 V, with a turn-on voltage close to 3V. The current efficiency reached 3.4 cd/A. Dendritic structures (**183** and **184**) were also studied as HTM for solution-processable devices (see Figure 13).[86] The two dendrimers showed an excellent solubility in most of the common organic solvents as well as a remarkable film-forming ability. T_g were determined as being of 115 °C for **183** and 140 °C for **184**, ensuring a sufficient stability for device fabrication. While examining their hole-transport ability in bilayer devices, a maximum luminance of 11 000 cd/m² and a maximum current efficiency of 4.01 cd/A were calculated for **184**-based devices. Comparison of the performances achieved with these dendrimers and benchmark HTMs indicated these dendrimers to be remarkable solution-processable candidates for OLEDs fabrication. Emitters were also designed with truxene.[87] As specificity, truxene, by its intrinsic blue emission, governed the emission colour prepared with it and imposed a blue emission to all emitters. Notably, the blue-emitting material **185** comprising anthracene side-groups furnished blue OLEDs in the following configuration: ITO / NPB (50 nm) / NPAT (40 nm) / TPBI (30 nm) / LiF (1 nm) / Al (100 nm). Devices exhibited a maximum current efficiency of 2.98 cd/A (at 6.2 V) with CIE (Commission Internationale de l'Eclairage)

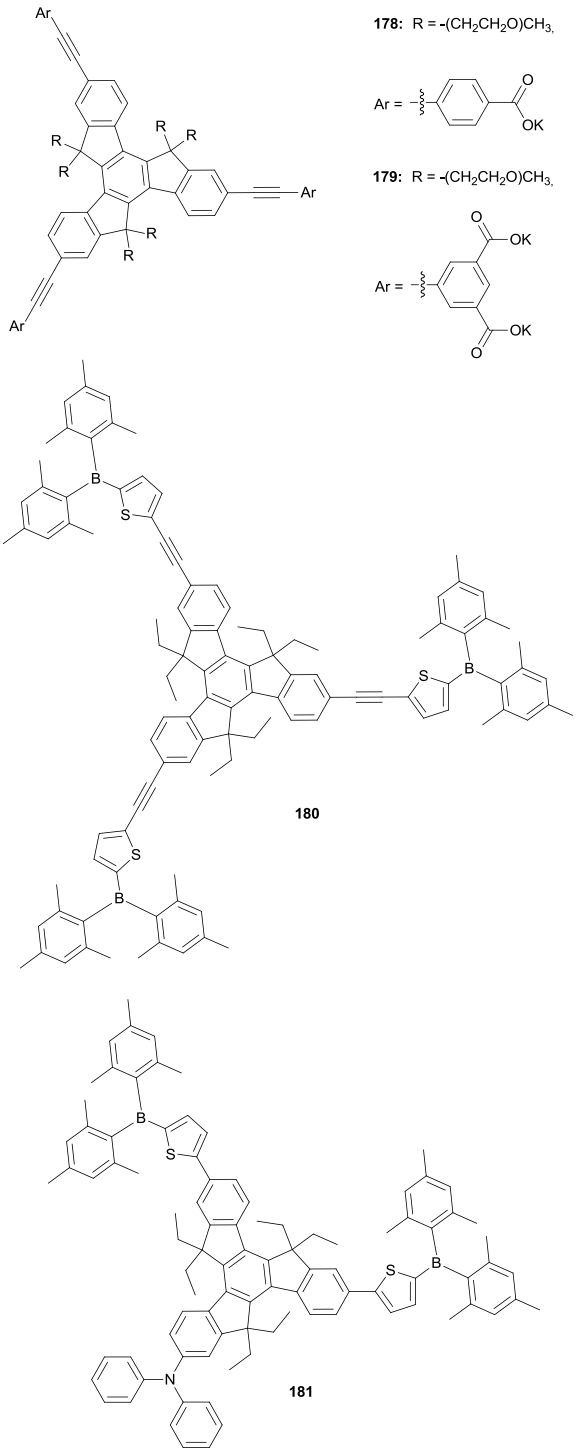

Figure 12. Fluorescent probes.

coordinates of (0.148, 0.138) and a maximum luminance of 1 318 cd/m². In a completely different approach, **97** was successfully used as an efficient colour converter for OLEDs.[88] More precisely, **97** was blended into a photoresist and subsequently inkjet printed on top of gallium nitride LEDs, modifying in turn the emission color.

3.6.2. Electrogenerated chemiluminescence

Another strategy to produce light is the electrogenerated chemiluminescence (ECL). Contrarily to the electroluminescence that consists in the injection of charges (holes and electrons) in the emissive layer to create excitons, electrochemiluminescence consists in generating light by electrochemical reactions in solution.[89] Notably, **97-98** and **108-109** produced stable radical anions and cations that gave blue ECLs by ion annihilation.[90] ECL intensity of **98** was especially high, around 80% of the intensity of the common blue ECL emitter 9,10-diphenylanthracene (DPA). Excepted **108** that showed an ECL emission at some longer wavelength of unknown origin, all compounds displayed an ECL emission superimposing their PL emission.

3.6.3. Organic Field-Effect Transistors (OFETs)

In the field of OFETs, the diversity of organic molecules remains still extremely limited as most of the π-conjugated molecules currently under investigation are all linear. To expand the scope of the molecules that can be tested and in order not to be only restricted to linear molecules, star-shaped materials were developed.[10,91] However, examples of semiconductors designed with truxene are scarce and only three molecules (**186-188**) have been reported in the same study (see Figure 14).[92] Device characteristics proved the mobility to be highly dependent of the number of thiophene rings in arms. Notably, elongation of the branches resulted in a transition from a polycrystalline to an amorphous state. The mobility decreased with increasing the number of thiophene units per branch. Mobility up to 1.03×10^{-3} $cm^2.V^{-1}.s^{-1}$ was however achieved with **186**, demonstrating the possibility to design semiconductors with truxene moiety. So far, this report constitutes the unique investigation of truxene as semiconductors for transistors.

3.6.4. Organic Photovoltaics (OPVs)

Truxene also proved to be a structure well-adapted for photovoltaic applications and this molecule was even suggested by some authors as the ideal π-conjugated core for the design of new star-shaped materials. Numerous sensitizers for dye sensitized solar cells (DSSC) and donating materials for solid state OPV cells were developed with truxene, mostly due to its excellent affinity for fullerenes. Indeed, compatibility of the sensitizer with the electron acceptor is a crucial parameter to optimize the electronic transfer. At least 17 structures (**189-197**) based on truxene were reported in the literature. For photovoltaic applications, the main parameters that govern the sensitizer efficacy are its strong absorption over the visible spectrum, a profitable mutual arrangement of both the donating and accepting groups to optimize the electronic transfer from the donor to the acceptor and finally the capacity of the sensitizer to be adsorbed at the surface of the TiO_2 electrode. Interestingly, bulkiness and rigidity of the truxene core could efficiently prevent from molecular aggregation of most of the materials studied in photovoltaics, what is essential, since the ultimate power output of the solar cells is intimately correlated with the control of the molecular organization at the nanoscale.

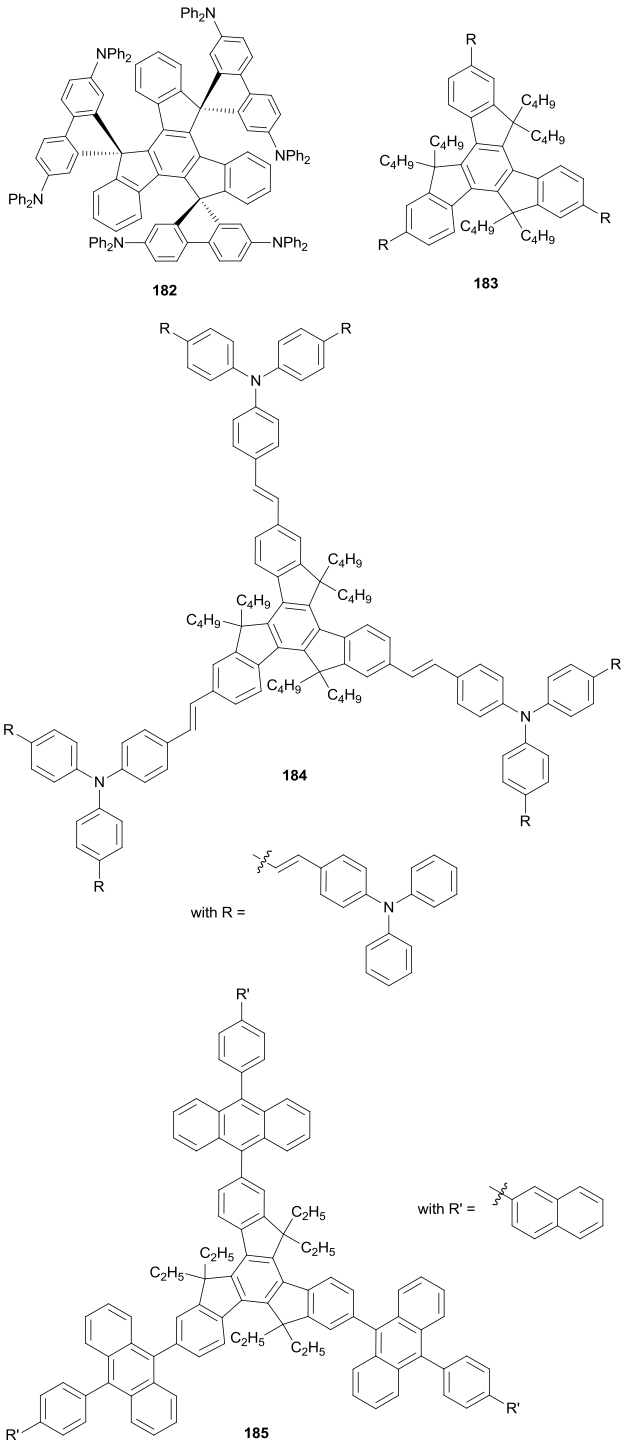

Figure 13. Hole-transport materials or emitters used in OLEDs.

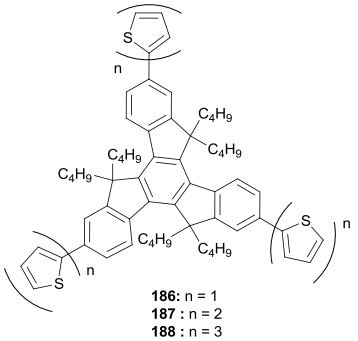

Figure 14. Semi-conductors **186-188** used in OFETs.

Numerous research groups worked on the design and synthesis of new organic dyes comprising the truxene moiety as the central core and peripheral triarylamine and cyanoacrylic acid groups as electron donating and electron accepting (anchoring groups) moieties respectively.[93] On the 17 structures reported so far, at least 9 dyes are based on the truxene/triarylamine combination. Generally, by introducing *n*-propyl chains at the inner-core position of truxene, disturbance of the π-π stacking was sufficient to prevent dyes from aggregating. This strategy was notably applied to **189-192** that comprise respectively a methine, thiophene, bithiophene or 3,4-ethylenedioxythiophene (EDOT) unit as rigid segment between the donor and the terminal cyanoacrylic acid group (see Figure 15).[93a] These dyes were found to significantly reduce the dark current in DSSC, leading in turn to enhanced performances.[94] As a result, high open circuit voltages (726-772 mV) were achieved. Best results were obtained with the high molar extinction coefficient dye **192** that yielded a maximum photon-to-current conversion efficiency (PCE) of 6.04%. Remarkable results with this dye can be assigned to the presence of the EDOT moiety well-known to be an excellent electron-donating group. Using **189** as a co-adsorbent for ruthenium dyes, PCE values of DSSCs could even be double compared to DSSCs only containing ruthenium dyes.[93b] Presence of **189** as a bulky co-adsorbent not only shielded the back electron transfer from the TiO_2 to I_3^- ions but also enhanced the light harvesting ability of the active layer in the short wavelength region. Considering the high PCE of 6.04% obtained with **192**, numerous derivatives of this dye were reported. New structures such as **193** (D−π−A), **194** 2(D−π−A) and **195** D−2(π−A) where D stands for donor, A for acceptor and π for conjugated spacer were developed.[93c] In iodine-free DSSCs, PCE of 7.2, 5.5 and 6.9% could be respectively obtained with **193-195**. By improving the electron donating ability of **192**, the two dyes **194** and **195** showed molar extinction coefficients outperforming those of **192** and even those of most of the common ruthenium dyes. However, only **195** gave a PCE higher than **192**. Still focusing on **192**, Hao *et al.* synthesized two sensitizers **196** and **197** varying from **192** by the position of the cyanoacrylic acid group.[95] This subtle modification induced a significant improvement of the short-circuit photocurrent density (J_{SC}) and thus of the PCE. Despites the presence of a stronger electron releasing group,

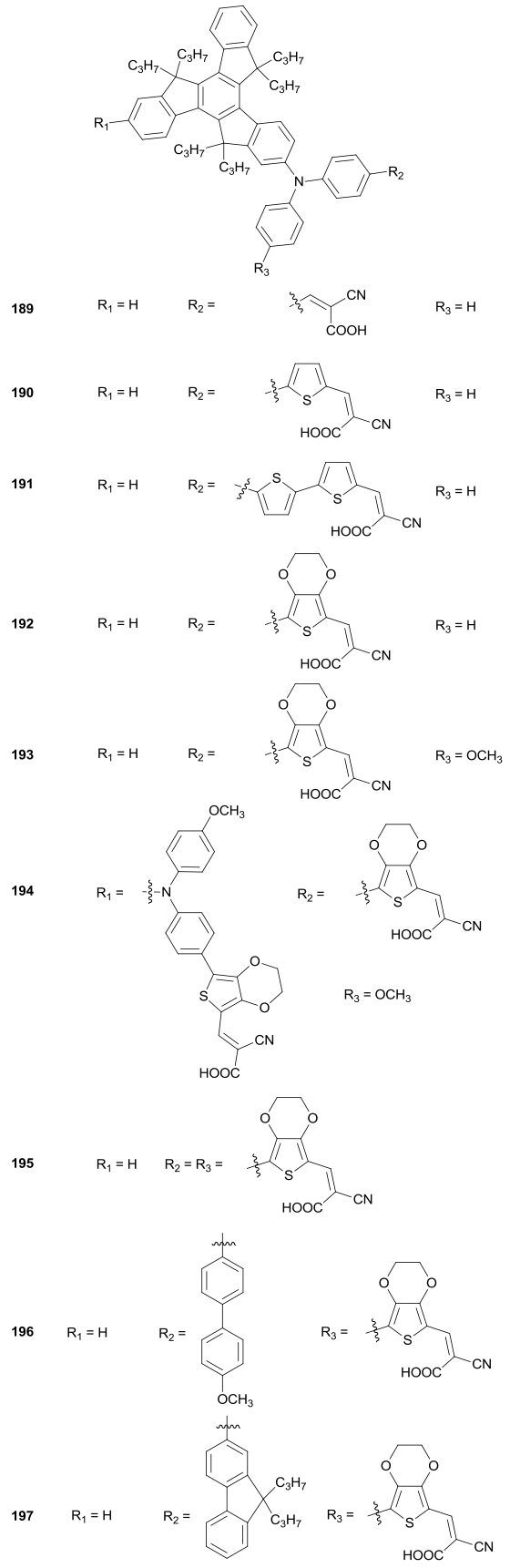

Figure 15. Truxenes derivatives **189-197** investigated in OPVs.

196 does not showed a better light harvesting ability than **197**. This unexpected behavior was assigned to the lower planarity of the conjugating system in **196** resulting from the presence of two consecutive phenyl rings. PCEs of DSSCs fabricated with these two dyes remained however higher than that obtained with **192**, ranging from 7.14 for **196** to 7.89% for **197** (and 6.67% for the reference devices fabricated with **192**). Till now, all mentioned dyes bearded an anchoring cyanoacrylic acid group. But dyes were also prepared without this group as exemplified with **198-202**.

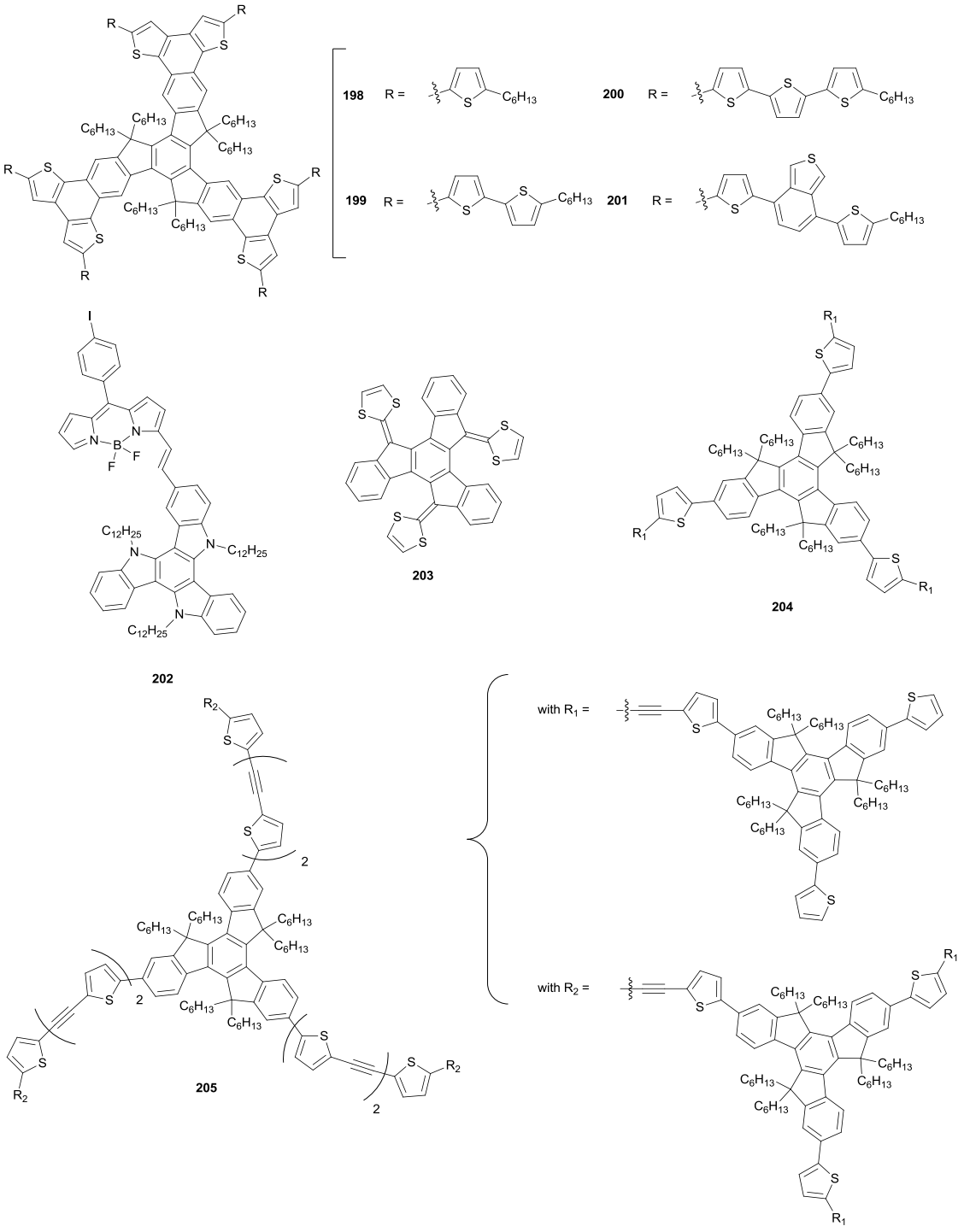

Figure 16. Dyes investigated in OPVs.

Notably, Yang *et al.*[96] reported a series of dyes comprising a truxene of extended aromaticity. The series of dyes **198-201** was especially designed so that their HOMO energy levels could be finely tuned, resulting in a gradual red-shift of their absorption maximum with the number of thiophene units (see Figure 16). A V_{OC} up to 1.07 V could be achieved with these dyes. Solar cells based on the **200**:$PC_{71}BM$ mixture (in a 1:3 ratio) displayed a PCE of 2.40% with a J_{SC} of 7.08 mA/cm^2. Recently, Ziessel's group developed a triazatruxene-functionalized Bodipy dye (**202**) that furnished the promising PCE of 0.9%.[97] The challenge was clearly to link the photosensititizer (Bodipy) to triazatruxene while keeping the charge carrier mobility. The *J-V* characteristics of devices showed a low fill factor, indicating that the charge carrier extraction was not efficient enough, even if an acceptable hole mobility was measured for the pure material (1×10^{-4} cm^2/V.s). As commonly observed, numerous dyes have also been developed for OPV applications without being in turn tested in the above-mentioned application. **203-205** belong to this category of molecules. For instance, concave bowl-shaped dye **203**, which possesses three proaromatic 1,3-dithiole rings, also exhibits a sphere-like geometry in perfect complementarity with the convex surface of C_{60}.[98] For high electron-donating ability, thiophenes can advantageously replace 1,3-dithiole rings, what was done with **204**, **205** and **206**. This strategy was logically extended to dendrimers. Based on truxene and thienyl-ethynylene units, dendrimers were synthesized by Wang *et al.* via a mixed divergent/convergent growth approach.[99] In particular, two dendritic structures containing up to four (**204**) and ten (**205**) thiophene-functionalized truxenes were prepared, with increasing the length of the thienylethynylene spacers at each generation. Such structures induced an intrinsic energy gradient from the periphery to the central truxene, resulting in a broad absorption over the UV-visible range. Evidence of the efficient energy transfer from the peripheral truxene moieties to the lower-energy center makes these dendrimers promising candidates for light harvesting materials. In the same spirit, by increasing the effective conjugation length between the central core and peripheral branches while tuning the ratio of acceptors (benzothiadiazole) and donors (triphenylamine), the same group successfully synthesized a D-π-A organic molecule (**206**) with a much broader absorption spectrum than that obtained with **204** and **205** (see Figure 17).[100] PCE of devices fabricated with the mixture of **206**/PCBM (1:3 w/w) as a photoactive layer was equal to 0.54%. In the former examples, C_{60} was mixed with the light harvesting materials. But they can also be linked together with a covalent bond. In this field, Guldi's group reported two light-harvesting dyads **207** and **208** differing by the distance between the two moities.[101] This distance exerted a notable impact on the photophysical features. Notably, thanks to the flexibility of the spacer, **208** adopted a spatially close geometry contrarily to **207** for which a larger distance between the two parts was observed. As a result, a stronger quenching of luminescence was observed for **208** than for **207** (i.e., toluene, 4×10^{-4} versus 1.2×10^{-3}). Proceeding further along the degree of charge transfer between the electron-donating and electron-accepting part, Wang *et al.* synthesized a series of star-shaped adducts **209-223**.[102] These adducts, which bear one to four C_{60} attached to truxene exhibited a remarkable thermal stability. While varying the π-linkages and the number of C_{60} moities, absorption and emission spectra of adducts could be finely tuned. Notably, investigation of the photophysical properties showed a significant decrease of the emission intensity upon increasing the number of C_{60} moities.

3.7. Liquid crystals and gels

3.7.1. Liquid crystals

The first report mentioning truxene-based liquid crystals was published in 1980 and several investigations were subsequently reported by the same group during the following years.[103,104] Typically, liquid crystals are made up of a rigid core joined together with flexible hydrocarbon chains.[105] Interestingly, several studies were devoted to study the same compounds that are rich in mesophases, namely **224**. However, the phase behaviours can differ significantly from one report to another one. Hence, Maliniak and coworkers reported **224** to be in a crystalline state up to 90°C, temperature at which a uniaxial discotic mesophase appears (see Figure 18). This liquid crystalline phase was determined as persisting until the clearing point at 191°C.[106] On the opposite, previous studies on the thermotropic behavior of **224** determined a more complicated behavior at low temperature with a first phase transition from solid to a columnar phase at 58°C, followed by the appearance of a nematic discotic phase at 67°C, an isotropic phase at 82°C, and a columnar phase at 89°C.[107] To get a deeper insight into the rheological properties of nematic phases, **225** that is structurally close to **224** was synthesized and the fluidity of the resulting phase could be determined as being Newtonian.[108] Interesting polymesomorphism of truxene-based liquid crystals have motivated the development of numerous *C_3*-symmetrical derivatives as exemplified with the series **226-229**.[109] In this series, the substitution pattern of the molecules strongly influenced the mesophase sequences. Thus, **227** only exhibited a highly ordered hexagonal columnar (Col_{ho}) mesophases over a broad range of temperature. On the opposite, **228** showed an inverted mesophase sequence of solid phase K→ discotic nematic phase N_D → columnar Col_h → isotropic I. And **229** displayed a reentrant N_D and Col_r mesophase. If **227-229** exhibited several poly-mesomorphisms, **226** showed only one Col_h mesophase, with a very high mesophase stability and a wide mesophase range. Finally, liquid crystals were also examined as materials for organic electronics. In this field, charge transport ability of **230** was clearly established.[110] A hole mobility in the order of 2×10^{-2} cm^2.V^{-1}.s^{-1} was determined for the hexagonal columnar (Col_h) mesophase, comparable to that obtained for amorphous Si. In a second study, this value increased until 10^{-1} cm^2.V^{-1}.s^{-1} at the Col_h - metastable phase transition.[111] These different studies clearly evidenced truxene to be an interesting molecular core for the

design of liquid crystalline semiconductors. In the same spirit, LCs can also be electro-active and a remarkable work in this field has been published in 2009.[112] As specificity, the peripheral aromatic rings were introduced to severely disrupt

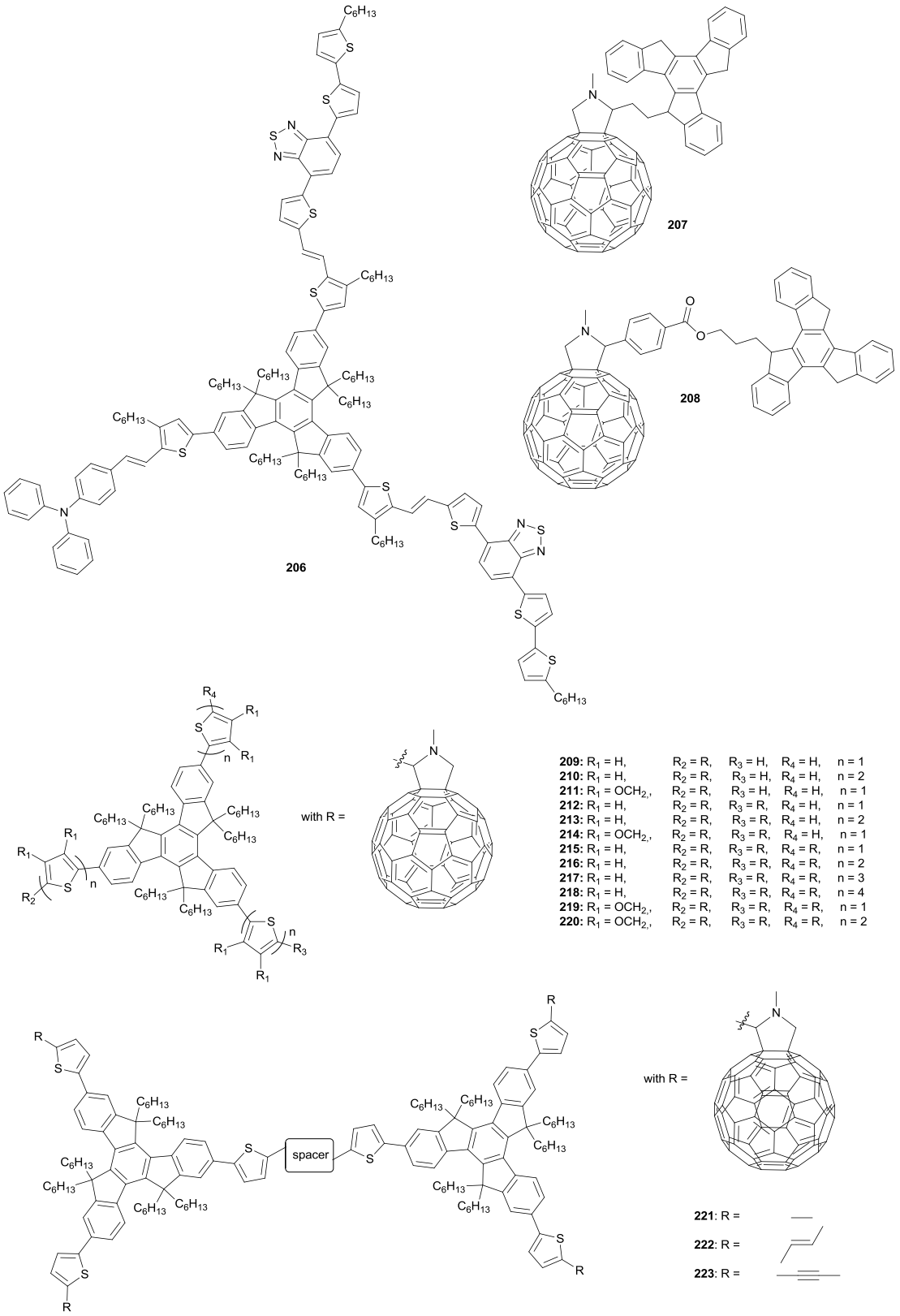

Figure 17. Truxenes derivatives investigated in OPVs

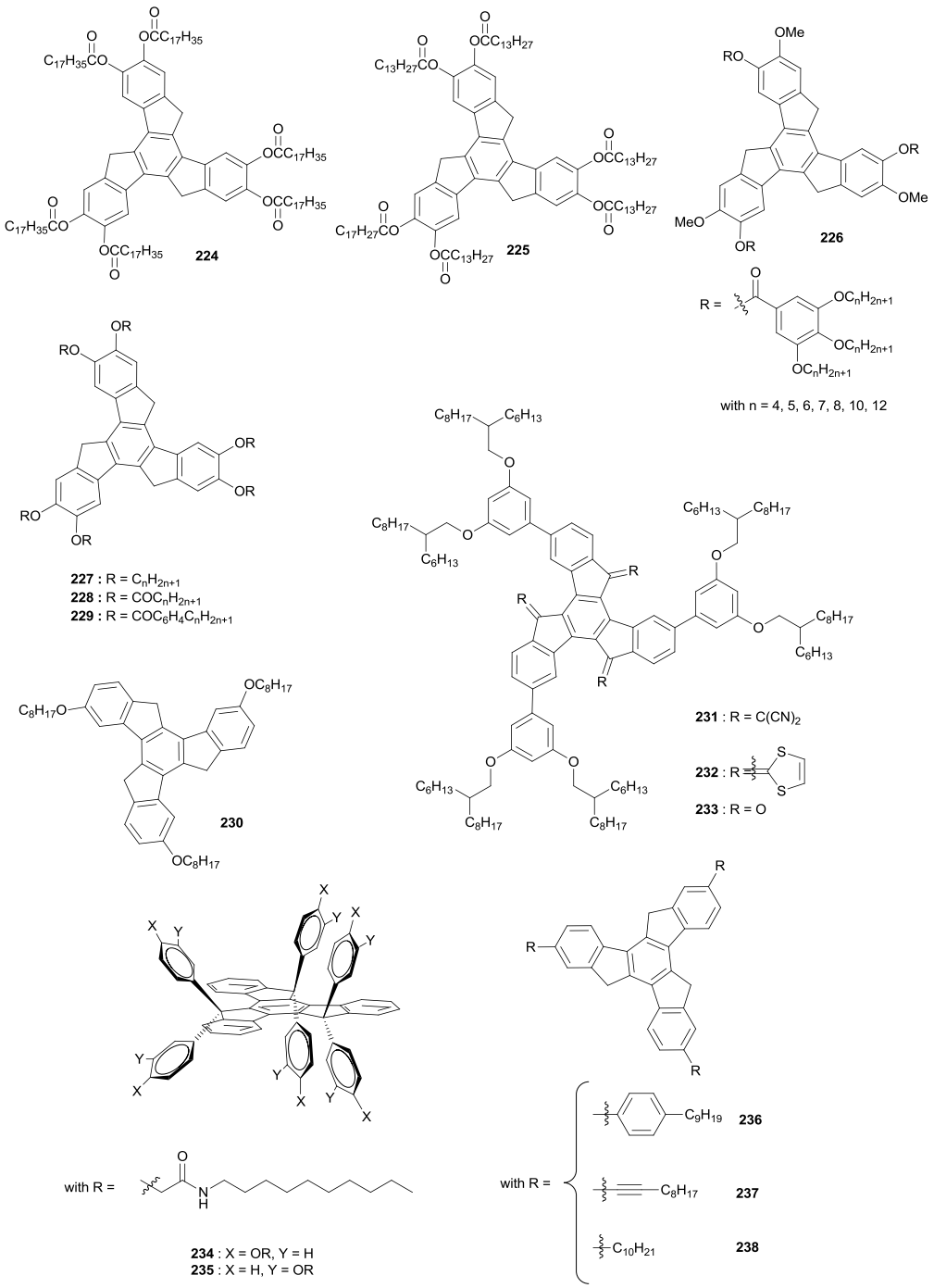

Figure 18. Truxene-based liquid crystals and truxene-based organogels.

the inter-disc attractions. By introducing dicyanomethylene substituents into the π-conjugated truxene framework, the resulting truxene derivative **231** showed a reversible four-step electrochemical reduction comparable to that observed for C_{60}.[113a] Especially, the first reduction process was observed at a less negative potential than that observed for C_{60}, indicative of the strong electron-accepting ability of **231.** Compound **233** also showed a three-step reduction process, but at higher potential, due to the lower accepting ability of ketone compared to dicyanomethylene. **231** and **233** were designed to exhibit reversible redox processes in reduction. But reversibility can also be observed in oxidation, as exemplified with **232**. Notably, **232** could show three reversible oxidation processes

thanks to the presence of three proaromatic 1,3-dithiole rings.[113b]

3.7.2. Organogels

To date, only few organogelators have been designed with polyaromatic disc-shaped molecules.[114] Here again, the substitution pattern strongly impacted the resulting supramolecular architecture that could be obtained and this phenomenon was clearly demonstrated with **234** and **235** (see Figure 18).[115] If the two gelators only vary by a subtle structural modification (substitution pattern of the peripheral groups of the truxene core), the difference of side-chain appendages induced a globular morphology for **234** and a fibrillar nano-morphology for **235**. Recently, remarkable gelation properties were reported for **236-238**.[116] Especially, introduction of a phenyl spacer between the central truxene core and the peripheral chains in **236** was determined as greatly improving the gelling ability of the system. As classically observed for gels, morphology of the xerogels formed with **236-238** proved to be highly solvent-dependent and nanostructures varying from interpenetrating networks made of flexible fibers and/or dense balls were obtained.

3.8. Optical applications

3.8.1. Non-Linear Optical applications

Because of their C_3-symmetry, a number of studies have been devoted to the exploitation of truxenone and related truxene derivatives as active materials for non-linear optical (NLO) applications. Their octupolar character combined to their polyaromaticity and their rigid planar skeleton is likely to result in more efficient NLO properties than the conventional dipolar molecules. As alternative to electro-optical media that are generally created by electric field poling, truxene-based chromophores could be simply aligned in thermally stable axially aligned chiral media.[117] Characterization of the NLO properties by Kleinman-disallowed hyper-Rayleigh scattering of **239-244** showed a significant enhancement of the unpolarized first hyperpolarizability values while improving the donating and/or the accepting ability of the substituents. Notably, if the hyperpolarizability values for **239** and **240** ranged from 212 to 247 × 10^{-30} esu, replacement of the linear amino groups by the cyclic pyrrolidine group enhanced the donating ability and improved the hyperpolarizability values (326 and 316 × 10^{-30} esu for **241** and **242** respectively). Similarly, at constant donating group, substitution of the carbonyls by dicyanomethylene groups caused a significant increase in the hyperpolarizabilities of the amino-derivatives (327 × 10^{-30} esu for **244** instead of 212 × 10^{-30} esu for **240**). Especially, these results outperformed the hyperpolarisability obtained with **243** (212 × 10^{-30} esu).[118]

3.8.2. Two-photon absorption

Numerous octupolar multi-branched derivatives were also studied for their two-photon absorption (TPA) properties. In the first work devoted to oligothiophenes attached to truxene, an increase by a factor 3 in the TPA cross section (σ_2) of **245-248** with respect to their isolated arms was observed.[119] This enhancement was assigned to the truxene core capable to efficiently separate the arms from each other, thus preventing from major through-space electronic interactions. More importantly, increase of the number of oligothiophene units strongly contributed to increase the TPA cross section. These trends were confirmed by other works devoted to **249-252**.[120] However, truxene contributed to reduce the TPA properties of **253-259** comprising platinum alkynyls complexes as peripheral groups (see Figure 20).[121]

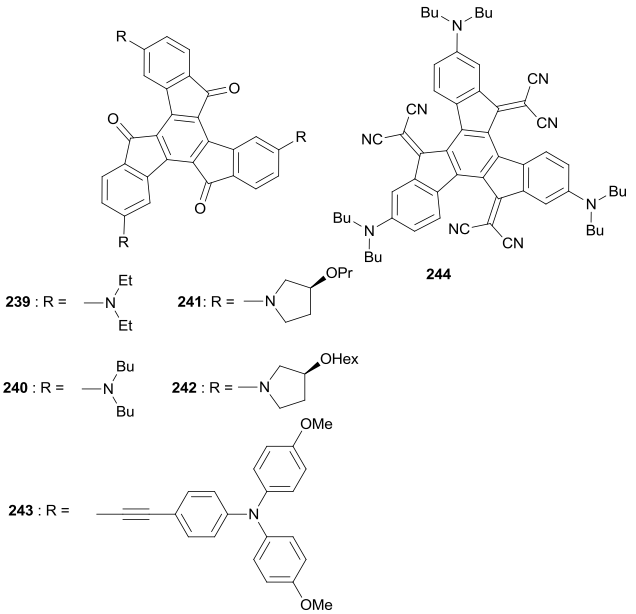

Figure 19. Truxenone and truxene derivatives investigated in NLO

3.9. Self-assembly and molecular wires

Truxene was also used to conceive two-dimensional monolayer structures on surface. These supramolecular networks were developed based on van der Waals and hydrogen bonding interactions. As the first examples, supramolecular networks on highly oriented pyrolyted graphite resulting from the self-assembly of **260** and **261** can be cited (see Figure 20).[122] If **260** and **261** self-assemble with the core parallel to the graphite surface, substitution at the inner-position also enforced these molecules to be adsorbed on graphite with an angle. Modification of the molecular arrangement with the substitution of the elemental building-block was also clearly demonstrated. Hence, a higher density of molecules per domains was observed for **261.** It lied in the fact that this molecule had a more marked tendency than **260** to stick together with the neighboring molecules by forming multi-hydrogen-bonds between tertriazine groups. If the former study mostly focused on the coverage density, the next one examined the diffusion behavior on surfaces.[123] In this aim, a custom designed molecule (5,10,15-*tris*(4-cyanophenyl-methyl)truxene

262) was synthesized and a nanoscale structured KBr(001) surface was used.

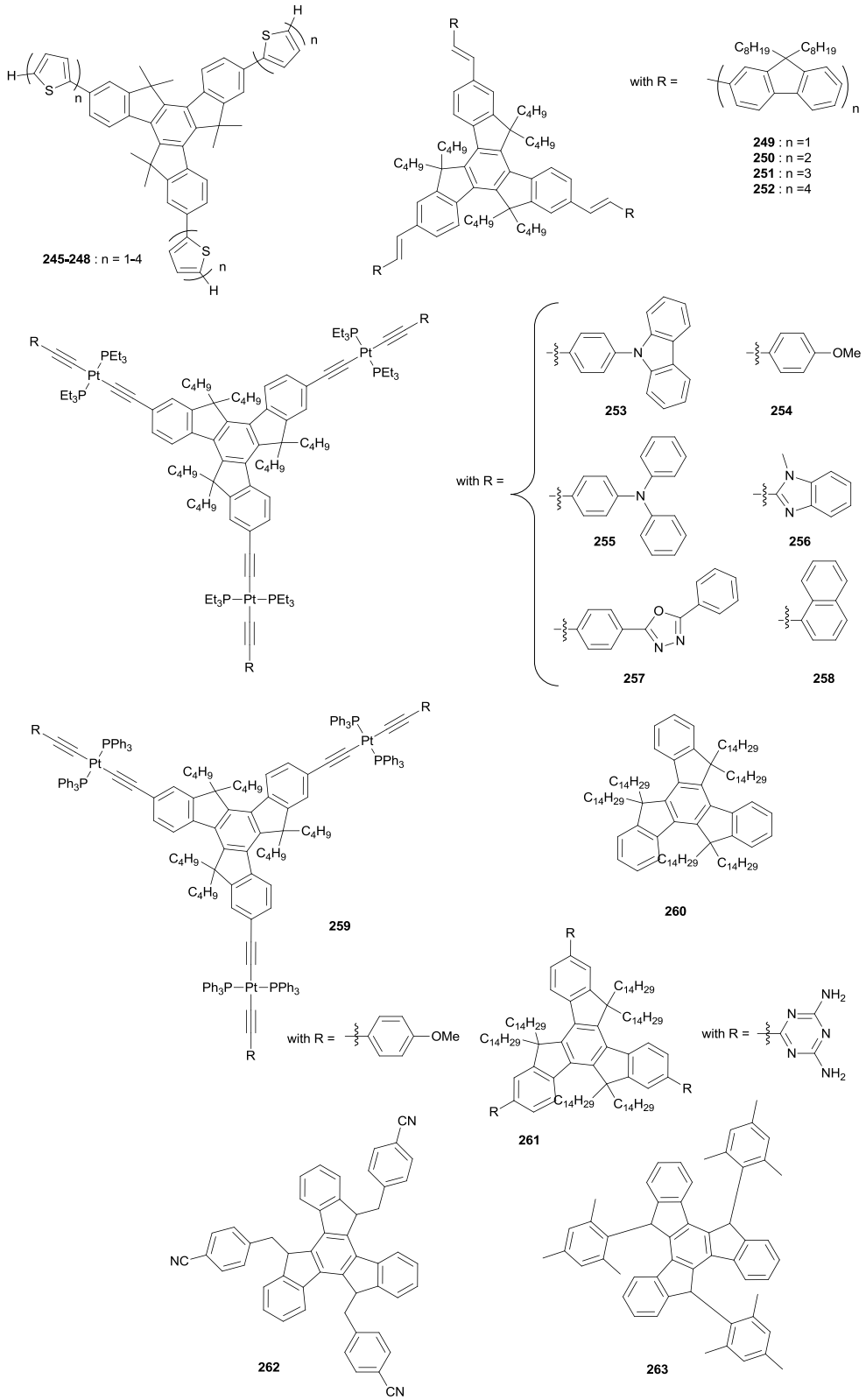

Figure 20. Truxene derivatives studied in Two-Photon Absorption and truxene-based supramolecular networks.

Examination of the diffusion behaviour of **262** at low coverages allowed the identification at least of three different regimes of molecular diffusion that could be theoretically simulated. Parallel to these works devoted to supramolecular networks, formation of covalent networks resulting from the in-situ formation of the truxene core by mean of cyclotrimerization was also studied. Tridimensional microporous ladder polymer networks with surface areas of up to 1650 m²/g were notably obtained.[124]

3.10. Dynamic nuclear polarization.

As a clearly emerging field of research is the dynamic nuclear polarization (DNP). As specificity, DNP is capable to boost the signal intensity of nuclear magnetic resonance (NMR) experiments, but also to deliver an unsurpassed sensitivity in numerous applications.[125] This method is based on the large polarization of a stable radical's unpaired electron that is subsequently transferred to proximal nuclei.[126] This approach was notably applied to EPR (Electron Paramagnetic Resonance) spectroscopy. To get narrow EPR line widths, the essential conditions are first the presence of quaternary carbons in the molecular structure but also a structure allowing a highly delocalized spin density shared by the quaternary carbons. These requirements were combined in the molecule **263** (see Figure 20).[127] Upon chemical reduction of **263**, the resulting truxene-based radical proved to be stable over several hours in solutions, even for solutions exposed to air but also to remain stable for months in the solid state under inert atmosphere. EPR analysis of **263** showed the line width at half height of the radical's maximum 140GHz EPR absorption to be 1.37 mT, broader than that of SA-BDPA (1.03 mT) and narrower than that of trityl OX063 (1.77 mT). It has to be notice that the comparison was established with two narrow line radicals well-known in DNP, evidencing the interest of the truxene-based DNP agent.

Conclusions

To conclude, over the years, the scope of applicability of truxene has been widely expanded thanks to the major breakthroughs achieved in the structural modifications of this PAH. A great deal of efforts has notably been devoted to render this structure soluble in most of the common organic solvents. This point being acquired,

Modification of the truxene core was thus possible. The full potential of truxene is now fully exploited in highly active research fields such as solar cells, organic transistors, organic diodes and two-photon absorption but also in emerging fields such as the dynamic nuclear polarization or the electro-generated chemiluminescence. For all these applications, researchers' imagination is the only limit since organic chemistry has long proven its versatility. The challenge for designing new materials with truxene is now open.

Notes and references

[a] Université de Cergy-Pontoise, Laboratoire de Physicochimie des Polymères et des Interfaces LPPI, 5 mail Gay Lussac, Neuville sur Oise, 95031 Cergy-Pontoise Cedex, France. E-mail: fabrice.goubard@u-cergy.fr; Fax: +33 1 34 25 70; Tel: +33 1 34 25 70 22

[b] Aix-Marseille Université, CNRS, Institut de Chimie radicalaire ICR, UMR 7273, F-13397 Marseille – France. E-mail: frederic.dumur@univ-amu.fr; Fax: +33 4 91 28 87 58; Tel: +33 4 91 28 27 48

1 F.S. Kipping, *J. Chem. Soc. Trans*., 1894, **65**, 269.
2 R. Seka and W. Kellermann, *Ber. dtsch. Chem. Ges. A/B*, 1942, **75**, 1730.
3 G. Metz, *Synthesis*, 1972, 614.
4 K.F. Lang, M. Zander and E.A. Theiling, *Chem. Ber*., 1960, **93**, 321.
5 K. Hartke and A. Schilling-Pindur, *Liebigs Ann. Chem*., 1984, **12**, 552.
6 J. Bergman and B. Egestad, *Chemica Scripta*, 1986, **26**, 287.
7 S.S. Elmorsy, A. Pelter, K. Smith, M.B. Hursthouse and D. Ando, *Tetrahedron Lett*., 1992, **33**, 821.
8 Y.N. Oded and I. Agranat, *Tetrahedron Lett*., 2014, **55**, 636.
9 O. de Frutos, B. Gomez-Lor, T. Granier, M.A. Monge, E. Gutierrez-Puebla and A.M. Echavarren, *Angew. Chem. Int. Ed*., 1999, **38**, 204.
10 J. Pei, J.-L. Wang, X.-Y. Cao, X.-H. Zhou and W.-B. Zhang, *J. Am. Chem. Soc*., 2003, **125**, 9944.
11 M.M. Boorum, Y.V. Vasil'ev, T. Drewello and L.T. Scott, *Science*, 2001, **294**, 828.
12 X.-Y. Cao, H. Zi, W. Zhang, H. Lu and J. Pei, *J. Org. Chem*., 2005, **70**, 3645.
13 E.V. Dehmlow and T. Kelle, *Synth. Commun*., 1997, **27**, 2021.
14 O. de Frutos, T. Granier, B. Gomez-Lor, J. Jimenez-Barbero, A. Monge, E. Gutierrez-Puebla and A.M. Echavarren, *Chem. Eur. J*., 2002, **8**, 2879.
15 M. Ruiz, B. Gomez-Lor, A. Santos and A.M. Echavarren, *Eur. J. Org. Chem*., 2004, 858.
16 B. Gómez-Lor, Ó. de Frutos and A.M. Echavarren, *Chem. Commun*., 1999, 2431.
17 B. Gomez-Lor, E. Gonzalez-Cantalapiedra, M. Ruiz, O. de Frutos, D. J. Cardenas, A. Santos and A.M. Echavarren, *Chem. Eur. J*., 2004, **10**, 2601.
18 N. Robertson, S. Parsons, E.J. MacLean, R.A. Coxall and A.R. Mount, *J. Mater. Chem*., 2000, **10**, 2043.
19 B. Gomez-Lor and A.M. Echavarren, *Org. Lett*., 2004, **6**, 2993.
20 E. González-Cantalapiedra, M. Ruiz, B. Gómez-Lor, B. Alonso, D. García-Cuadrado, D.J. Cárdenas and A.M. Echavarren, *Eur. J. Org. Chem*., 2005, 4127.
21 B. Gomez-Lor, O. de Frutos, P.A. Ceballos, T. Granier and A.M. Echavarren, *Eur. J. Org. Chem*., 2001, 2107.
22 J.-S. Yang, Y.-R. Lee, J.-L. Yan and M.-C. Lu, *Org. Lett*., 2006, **8**, 5813.
23 A.H. Abdourazak, Z. Marcinow, A. Sygula, R. Sygula and P.W. Rabideau, *J. Am. Chem. Soc*., 1995, **117**, 6410.
24 L.T. Scott, M.M. Boorum, B.J. McMahon, S. Hagen, J. Mack, J. Blank, H. Wegner and A. de Meijere, *Science*, 2002, **295**, 1500.
25 Y. Xie, X. Zhang, Y. Xiao, Y. Zhang, F. Zhou, J. Qi and J. Qu, *Chem. Commun*., 2012, **48**, 4338.

26 M.-T. Kao, J.-H. Chen, Y.-Y. Chu, K.-P. Tseng, C.-H. Hsu, K.-T. Wong, C.-W. Chang, C.-P. Hsu and Y.-H. Liu, *Org. Lett*., 2011, **13**, 1714.

27 J. Kim, Y.K. Kim, N. Park, J.H. Hahn and K.H. Ahn, *J. Org. Chem*., 2005, **70**, 7087.

28 B. Gomez-Lor, G. Hennrich, B. Alonso, A. Monge, E. Gutierrez-Puebla and A.M. Echavarren, *Angew. Chem. Int. Ed*., 2006, **45**, 4491.

29 a) G.R. Newkome, C.N. Moorefield and F. Vögtle, *Dendritic Molecules: Concepts, Synthesis, Perspectives*; Wiley-VCH: Weinheim, Germany, 2002; b) J.M.J. Fréchet and D.A. Tomalia, *Dendrimers and Other Dendritic Polymers*; Wiley: Chichester, U. K., 2001.

30 a) X.-Y. Cao, W.-B. Zhang, J.-L. Wang, X.-H. Zhou, H. Lu and J. Pei, *J. Am. Chem. Soc*., 2003, **125**, 12430; b) X.-Y. Cao, X.-H. Liu, X.-H. Zhou, Y. Zhang, Y. Jiang, Y. Cao, Y.-X. Cui and J. Pei, *J. Org. Chem*., 2004, **69**, 6050.

31 W.-B. Zhang, W.-H. Jin, X.-H. Zhou and J. Pei, *Tetrahedron*, 2007, **63**, 2907.

32 a) A.L. Kanibolotsky, R. Berridge, P.J. Skabara, I.F. Perepichka, D.D.C. Bradley and M. Koeberg, *J. Am. Chem. Soc*., 2004, **126**, 13695; b) W.-Y. Lai, D. Liu and W. Huang, *Macromol. Chem. Phys*., 2011, **212**, 445; c) N. Thomson, A.L. Kanibolotsky, J. Cameron, T. Tuttle, N.J. Findlay and P.J. Skabara, *Beilstein J. Org. Chem*., 2013, **9**, 1243; d) Q. Chen, F. Liu, Z. Ma, B. Peng, W. Wei and W. Huang, *Synlett*, 2007, **20**, 3145; e) M.M. Oliva, J. Casado, J.T. Lopez Navarrete, R. Berridge, P.J. Skabara, A.L. Kanibolotsky and I.F. Perepichka, *J. Phys. Chem. B*, 2007, **111**, 4026; f) Q.-Q. Chen, F. Liu, Z. Ma, B. Peng, W. Wei and W. Huang, *Chem. Lett*., 2008, **37**, 178; g) S.-C. Yuan, Q. Sun, T. Lei, B. Du, Y.-F. Li and J. Pei, *Tetrahedron*, 2009, **65**, 4165; h) W.-Y. Lai, R. Xia, D.D.C. Bradley and W. Huang, *Chem. Eur. J*., 2010, **16**, 8471; i) M. Fujitsuka, D.W. Cho, H.-H. Huang, J.-S. Yang and T. Majima, *J. Phys. Chem. B*, 2011, **115**, 13502; j) M. Fujitsuka, S. Tojo, J.-S. Yang and T. Majima, *Chem. Phys*., 2013, **419**, 118; k) Y.-H. Wang, J.-Q. Hou, Z.-H. Kang, L.-J. Gong, T.-H. Huang, L.-L. Qu, Y.-G. Ma, R. Lu and H.-Z. Zhang, *Chem. Phys. Lett*., 2013, **566**, 17; l) M. Fujitsuka, D.W. Cho, H.-H. Huang, J.-S. Yang and T. Majima, *J. Phys. Chem. B*, 2013, **117**, 2828.

33 H. Xia, J. He, B. Xu, S. Wen, Y. Li and W. Tian, *Tetrahedron*, 2008, **64**, 5736.

34 L. Wang, Y. Jiang, J. Luo, Y. Zhou, J.H. Zhou, J. Wang and J. Pei, *Adv. Mater*., 2009, **47**, 4854.

35 J.-L. Wang, Y.-T. Chan, C.N. Moorefield, J. Pei, D.A. Modarelli, N.C. Romano and G.R. Newkome, *Macromol. Rapid Commun*., 2010, **31**, 850.

36 B. Du, S.-C. Yuan and J. Pei, *Aust. J. Chem*., 2011, **64**, 1211.

37 B. Du, D. Fortin and P.D. Harvey, *Inorg. Chem*., 2011, **50**, 11493.

38 X.-Y. Cao, X.-H. Zhou, H. Zi and J. Pei, *Macromolecules*, 2004, **37**, 8874.

39 a) J. Huber, K. Müllen, J. Salbeck, H. Schenk, U. Scherf, T. Stehlin and R. Stern, *Acta Polym*., 1994, **45**, 244; b) U. Lemmer, S. Heun, R.F. Mahrt, U. Scherf, M. Hopmeier, U. Sieger, E.O. Göbel, K. Müllen and H. Bässler, *Chem. Phys. Lett*., 1995, **240**, 373; c) M. Grell, D.D.C. Bradley, G. Ungar, J. Hill and K.S. Whitehead, *Macromolecules* 1999, **32**, 5810; d) S.A. Jenekhe and J.A. Osaheni, *Science*, 1994, **265**, 765; e) X. Gong, P.K. Iyer, D. Moses, G.C. Bazan, A.J. Heeger and S.S. Xiao, *Adv. Funct. Mater*., 2003, **13**, 325; f) U. Scherf and E.J.W. List, *Adv. Mater*., 2002, **14**, 477.

40 a) J. Pina, J.S. Seixas de Melo, J.-M. Koenen, S. Jung and U. Scherf, *J. Phys. Chem. C*, 2013, **117**, 3718; b) J.-M. Koenen, S. Jung, A. Patra, A. Helfer and U. Scherf, *Adv. Mater*., 2012, **24**, 681.

41 D. Li, X. Wang, J. Xin, W. Yutao, W. Aiqing and Y. Wu, *Chin. J. Chem*., 2012, **30**, 861.

42 a) P. Xiao, J. Zhand, F. Dumur, M.A. Tehfe, F. Morlet-Savary, B. Graff, D. Gigmes, J.-P. Fouassier and J. Lalevée, *Progress Polym. Sci.*, 2014, 10.1016/j.progpolymsci.2014.09.001 b) J. Lalevée, M.-A. Tehfe, F. Dumur, D. Gigmes, B. Graff, F. Morlet-Savary and J.-P. Fouassier, *Macromol. Rapid Commun*., 2013, **34**, 239.

43 M.-A. Tehfe, F. Dumur, B. Graff, J.-L. Clément, D. Gigmes, F. Morlet-Savary, J.-P. Fouassier and J. Lalevée, *Macromolecules*, 2013, **46**, 736.

44 M.-A. Tehfe, F. Dumur, E. Contal, B. Graff, D. Gigmes, J.-P. Fouassier and J. Lalevée, *Macromol. Chem. Phys*., 2013, **214**, 2189.

45 M.-A. Tehfe, J. Lalevée, S. Telitel, E. Contal, F. Dumur, D. Gigmes, D. Bertin, M. Nechab, B. Graff, F. Morlet-Savary and J.-P. Fouassier, *Macromolecules*, 2012, **45**, 4454.

46 B. Guilhabert, N. Laurand, J. Herrnsdorf, Y. Chen, A.R. Mackintosh, A.L Kanibolotsky, E. Gu, P.J. Skabara, R.A. Pethrick and M.D. Dawson, *J. Opt*., 2010, **12**, 035503.

47 a) N. Grassie and G. Scott, *Polymer Degradation and Stabilisation*, Cambridge University Press, 1985; b) W. Zhao, T. Cao and J.M. White, *Adv. Funct. Mater*., 2004, **14**, 783; c) L. Cerdán, A. Costela, G. Durán-Sampedro, I. García-Moreno, M. Calle, M. Juan-y-Seva, J. de Abajo and G. A. Turnbull, *J. Mater. Chem*., 2012, **22**, 8938.

48 K. Kreger, M. Bäte, C. Neuber, H.-W. Schmidt and P. Strohriegl, *Adv. Funct. Mater*., 2007, **17**, 3456.

49 S. Hattori, A. Yamada, S. Saito, K. Asakawa, T. Koshiba and T. Nakasugi, *J. Photopolym. Sci. Technol*., 2009, **22**, 609.

50 a) C. Foucher, B. Guilhabert, A.L. Kanibolotsky, P.J. Skabara, N. Laurand and M.D. Dawson, *Opt. Mater. Express*, 2013, **3**, 584; b) Y. Wang, G. Tsiminis, Y. Yang, A. Ruseckas, A.L. Kanibolotsky, I.F. Perepichka, P.J. Skabara, G.A. Turnbull and I.D.W. Samuel, *Synth. Met*., 2010, **160**, 1397.

51 G. Tsiminis, Y. Wang, P.E. Shaw, A.L. Kanibolotsky, I.F. Perepichka, M.D. Dawson, P.J. Skabara, G.A. Turnbull and I.D.W. Samuel, *Appl. Phys. Lett*., 2009, **94**, 243304.

52 A.-M. Haughey, B. Guilhabert, A.L. Kanibolotsky, P.J. Skabara, G.A. Burley, M.D. Dawson and N. Laurand, *Sens. Actuators B*, 2013, **185**, 132.

53 K.F. Lang, M. Zander and E.A. Theiling, *Ber*., 1960, **93**, 321.

54 D. Baunsgaard, N. Harrit, M. El Balsami, F. Negri, G. Orlandi, J. Frederiksen and R. Wilbrandt, *J. Phys. Chem. A*, 1998, **102**, 10007.

55 X. Zhou, A.-M. Rena and J.-K. Feng, *Polymer*, 2004, **45**, 7747.

56 J.-S. Yang, H.-H. Huang and J.-H. Ho, *J. Phys. Chem. B*, 2008, **112**, 8871.

57 N.A. Montgomery, J.-C. Denis, S. Schumacher, A. Ruseckas, P.J. Skabara, A. Kanibolotsky, M.J. Paterson, I. Galbraith, G.A. Turnbull and I.D.W. Samuel, *J. Phys. Chem. A*, 2011, **115**, 2913.

58 a) S. Schumacher, A. Ruseckas, N.A. Montgomery, P.J. Skabara, A.L. Kanibolotsky, M.J. Paterson, I. Galbraith, G.A. Turnbull, I.D.W. Samuel, *J. Chem. Phys*., 2009, **131**, 154906; b) E. Jansson, P.C. Jha, H. Agren, *Chem. Phys*., 2007, **336**, 91.

59 N.A. Montgomery, G.J. Hedley, A. Ruseckas, J.-C. Denis, S. Schumacher, A.L. Kanibolotsky, P.J. Skabara, I. Galbraith, G.A. Turnbull and I.D.W. Samuel, *Phys. Chem. Chem. Phys*., 2012, **14**, 9176.
60 C.R. Belton, A.L. Kanibolotsky, J. Kirkpatrick, C. Orofino, S.E.T. Elmasly, P.N. Stavrinou, P.J. Skabara and D.D.C. Bradley, *Adv. Funct. Mater*., 2013, **23**, 2792.
61 W.-B. Zhang, W.-H. Jin, X.-H. Zhou and J. Pei, *Tetrahedron*, 2007, **63**, 2907.
62 a) M.-S. Yuan, Q. Wang, W.-J. Wang, T.-B. Li, L. Wang, W. Deng, Z.-T Du and J.-R. Wang, *Dyes Pigments*, 2012, **95**, 236; b) M.-S. Yuan, Q. Fang, Y.-R. Zhang and Q. Wang, *Spectrochim. Acta A*, 2011, **79**, 1112.
63 R. Misra, R. Sharma and S.M. Mobin, *Dalton Trans*., 2014, **43**, 6891.
64 a) X.-Y. Cao, W. Zhang, H. Zi and J. Pei, *Org. Lett*., 2004, **6**, 4845; b) J.-L. Wang, Z.-M. Tang, Q. Xiao, Q.-F. Zhou, Y. Ma and J. Pei, *Org. Lett*., 2008, **10**, 17.
65 X.-F. Duan, J.-L. Wang and J. Pei, *Org. Lett*., 2005, **7**, 4071.
66 M.-S. Yuan, Q. Fang, Z.-Q. Liu, J.-P. Guo, H.-Y. Chen, W.-T. Yu, G. Xue and D.-S. Liu, *J. Org. Chem*., 2006, **71**, 7858.
67 M.-S. Yuan, Z.-Q. Liu and Q. Fang, *J. Org. Chem*., 2007, **72**, 7915.
68 Q. Zheng, G.S. He and P.N. Prasad, *Chem. Mater*., 2005, **17**, 6004.
69 a) S. Diring and R. Ziessel, *Tetrahedron Lett*., 2009, **50**, 1203; b) S. Diring, F. Puntoriero, F. Nastasi, S. Campagna and R. Ziessel, *J. Am. Chem. Soc*., 2009, **131**, 6108.
70 Y. Xie, X. Zhang, Y. Xiao, Y. Zhang, F. Zhou, J. Qi and J. Qu, *Chem. Commun*., 2012, **48**, 4338.
71 S. Diring, R. Ziessel, F. Barigelletti, A. Barbieri and B. Ventura, *Chem. Eur. J*., 2010, **16**, 9226.
72 C. Chiorboli, C.A. Bignozzi, F. Scandola, E. Ishow, A. Gourdon and J.P. Launay, *Inorg. Chem*., 1999, **38**, 2402.
73 B. Ventura, A. Barbieri, F. Barigelletti, S. Diring and R. Ziessel, *Inorg. Chem*., 2010, **49**, 8333.
74 S. Diring, B. Ventura, A. Barbieri and R. Ziessel, *Dalton Trans*., 2012, **41**, 13090.
75 B. Du and P.D. Harvey, *Chem. Commun*., 2012, **48**, 2671.
76 B. Du, D. Fortin and P.D. Harvey, *J. Inorg. Organomet. Polym*., 2013, **23**, 81.
77 J.-Y. Wang, J. Yan, L. Ding, Y. Ma and J. Pei, *Adv. Funct. Mater*., 2009, **19**, 1746.
78 J. Zhang, R.E. Campbell, A.Y. Ting and R.Y. Tsien, *Nat. Rev. Mol. Cell Biol*., 2002, **3**, 906.
79 Y. Chen, C. Zhu, Z. Yang, J. Chen, Y. He, Y. Jiao, W. He, L. Qiu, J. Cen and Z. Guo, *Angew. Chem. Int. Ed*., 2013, **52**, 1688.
80 N. Earmrattana, M. Sukwattanasinitt and P. Rashatasakhon, *Dyes Pigments*, 2012, **93**, 1428.
81 A.-M. Haughey, B. Guilhabert, A. Kanibolotsky, P.J. Skabara, M.D. Dawson, G.A. Burley and N. Laurand, *Biosens. Bioelectron*., 2014, **54**, 679.
82 M.-S. Yuan, Q. Wang, W. Wang, D.-E. Wang, J. Wang and J. Wang, *Analyst*, 2014, **139**, 1541.
83 C.W. Tang and S.A. VanSlyke, *Appl. Phys. Lett*., 1987, **51**, 913.
84 a) J. Li, T. Zhang, Y. Liang and R. Yang, *Adv. Funct. Mater*., 2013, **23**, 619; b) Y. Tao, C. Yang and J. Qin, *Chem. Soc. Rev*., 2011, **40**, 2943.
85 M. Kimura, S. Kuwano, Y. Sawaki, H. Fujikawa, K. Noda, Y. Taga and K. Takagi, *J. Mater. Chem*., 2005, **15**, 2393.
86 Z. Yang, B. Xu, J. He, L. Xue, Q. Guo, H. Xia and W. Tian, *Org. Electron*., 2009, **10**, 954.
87 J. Huang, B. Xu, J.-H. Su, C.H. Chen and H. Tian, *Tetrahedron*, 2010, **66**, 7577.
88 M. Wu, Z. Gong, A.J.C. Kuehne, A.L. Kanibolotsky, Y.J. Chen, I.F. Perepichka, A.R. Mackintosh, E. Gu, P.J. Skabara, R.A. Pethrick and M.D. Dawson, *Opt. Express*, 2009, **17**, 16436.
89 R.J. Forster, P. Bertoncello and T.E. Keyes, *Annu. Rev. Anal. Chem*. 2009, **2**, 359.
90 K.M. Omer, A.L. Kanibolotsky, P.J. Skabara and I.F. Perepichka and A. J. Bard, *J. Phys. Chem. B*, 2007, **111**, 6612.
91 a) Y. Nicolas, P. Blanchard, E. Levillain, M. Allain, N. Mercier and J. Roncali, *Org. Lett*., 2004, **6**, 273 ; b) M. Kimera, H. Narikawa, K. Ohta, K. Hanabusa, H. Shirai and N. Kobayashi, *Chem. Mater*., 2002, **14**, 2711.
92 Y. Sun, K. Xiao, Y. Liu, J. Wang, J. Pei, G. Yu and D. Zhu, *Adv. Funct. Mater*., 2005, **15**, 818.
93 a) M. Liang, M. Lu, Q.-L. Wang, W.-Y. Chen, H.-Y. Han, Z. Sun and S. Xue, *J. Power Sources*, 2011, **196**, 1657; b) Y. Shi, M. Liang, L. Wang, H. Han, L. You, Z. Sun and S. Xue, *ACS Appl. Mater. Interfaces*, 2013, **5**, 144; c) X. Zong, M. Liang, C. Fan, K. Tang, G. Li, Z. Sun and S. Xue, *J. Phys. Chem. C*, 2012, **116**, 11241; d) X. Zong, M. Liang, T. Chen, J. Jia, L. Wang, Z. Sun and S. Xue, *Chem. Commun*., 2012, **48**, 6645; e) G.V. Baryshnikov, B.F. Minaev, V.A. Minaeva, Z. Ning and Q. Zhang, *Optics Spectrosc*., 2012, **112**, 168.
94 a) D.P. Hagberg, T. Marinado, K.M. Karlsson, K. Nonomura, P. Qin, G. Boschloo, T. Brinck, A. Hagfeldt and L. Sun, *J. Org. Chem*., 2007, **72**, 9550; b) W.-H. Liu, I.-C. Wu, C.-H. Lai, C.-H. Lai, P.-T. Chou, Y.-T. Li, C.-L. Chen, Y.-Y. Hsu and Y. Chi, *Chem. Commun*., 2008, 5152.
95 a) Y. Hao, M. Liang, Z. Wang, L. Wang, Y. Sun, Z. Sun and S. Xue, *Phys. Chem. Chem. Phys*., 2013, **15**, 15441; b) Y. Hao, M. Liang, Z. Wang, F. Cheng, C. Wang, Z. Sun and S. Xue, *Tetrahedron*, 2013, **69**, 10573.
96 X. Yang, Q. Zheng, C. Tang, D. Cai, S.-C. Chen and Y. Ma, *Dyes Pigments*, 2013, **99**, 366.
97 T. Bura, N. Leclerc, S. Fall, P. Leveque, T. Heiser and R. Ziessel, *Org. Lett*., 2011, **13**, 6030.
98 E.M. Perez, M. Sierra, L. Sanchez, M.R. Torres, R. Viruela, P.M. Viruela, E. Orti and N. Martin, *Angew. Chem. Int. Ed*., 2007, **46**, 1847.
99 J.-L. Wang, J. Luo, L.-H. Liu, Q.-F. Zhou, Y. Ma and J. Pei, *Org. Lett*., 2006, **8**, 2281.
100 J.-L. Wang, Z. He, H. Wu, H. Cui, Y. Li, Q. Gong, Y. Cao and J. Pei, *Chem. Asian J*., 2010, **5**, 1455.
101 L. Sanchez, N. Martin, E. Gonzalez-Cantalapiedra, A.M. Echavarren, G.M. Aminur Rahman and D.M. Guldi, *Org. Lett*., 2006, **8**, 2451.
102 J.-L. Wang, X.-F. Duan, B. Jiang, L.-B. Gan and J. Pei, *J. Org. Chem*., 2006, **71**, 4400.
103 a) C. Destrade, J. Malthete, N.H. Tinh and H. Gasparoux, *Phys. Lett*., 1980, **78A**, 82; b) N.H. Tinh, J. Malthete and C. Destrade, *J. Phys. Lett*., 1981, **42**, L417; c) C. Destrade, P. Foucher, J. Malthete and N.H. Tinh, *Phys. Lett*., 1982, **88A**, 187.

104 C. Destrade, P. Foucher, H. Gasparoux, N.H. Tinh, A.M. Levelut and J. Malthete, *Mol. Cryst. Liq. Cryst*., 1984, **106**, 121.
105 E. Fontes, P.A. Heiney, M. Ohba, J.N. Haseltine and A.B. Smith III, *Phys. Rev. A*, 1988, **37**, 1329.
106 D. Sandström, M. Nygren, H. Zimmermann and A. Maliniak, *J. Phys. Chem*., 1995, **99**, 6661.
107 a) T. Warmerdam, D. Frenkel and R.J.J. Zijlstra, *Liq. Cryst*., 1988, **3**, 149; b) T.W. Warmerdam, R.J.M. Nolte, W. Drenth, J.C. van Miltenburg, D. Frenkel and R.J.J. Ziilstra, *Liq. Cryst*., 1988, **3**, 1087.
108 K. Negita, C. Kawano and K. Moriya, *Phys. Rev. E*, 2004, **70**, 021702.
109 L.-L. Li, P. Hu, B.-Q. Wang, W.-H. Yu, Y. Shimizu and K.-Q. Zhao, *Liq. Cryst*., 2010, **37**, 499.
110 K.-Q. Zhao, C. Chen, H. Monobe, P. Hu, B.-Q. Wang and Y. Shimizu, *Chem. Commun*., 2011, **47**, 6290.
111 H. Monobe, C. Chen, K.-Q. Zhao, P. Hu, Y. Miyake, A. Fujii, M. Ozaki and Y. Shimizu, *Mol. Cryst. Liq. Cryst*., 2011, **545**, 149/[1373]-155/[1379].
112 K. Isoda, T. Yasuda and T. Kato, *Chem. Asian J*., 2009, **4**, 1619.
113 a) Q. Xie, E. Pérez-Cordero and L. Echegoyen, *J. Am. Chem. Soc*., 1992, **114**, 3978; b) H. Isla, B. Grimm, E.M. Perez, M. Rosario Torres, M.Angeles Herranz, R. Viruela, J. Arago, E. Orti, D. M. Guldi and N. Martın, *Chem. Sci*., 2012, **3**, 498.
114 T. Ishi-I, T. Hirayama, K.-I. Murakami, H. Tashiro, T. Thiemann, K. Kubo, A. Mori, S. Yamasaki, T. Akao, A. Tsuboyama, T. Mukaide, K. Ueno and S. Mataka, *Langmuir*, 2005, **21**, 1261.
115 K.-P. Tseng, M.-T. Kao, T.W.T. Tsai, C.-H. Hsu, J.C.C. Chan, J.-J. Shyue, S.-S. Sun and K.-T. Wong, *Chem. Commun*., 2012, **48**, 3515.
116 S. Gomez-Esteban, M. Pezella, A. Domingo, G. Hennrich and B. Gomez-Lor, *Chem. Eur. J*., 2013, **19**, 16080.
117 L. Sanguinet, J.C. Williams, Z. Yang, R.J. Twieg, G. Mao, K.D. Singer, G. Wiggers and R.G. Petschek, *Chem. Mater*., 2006, **18**, 4259.
118 C. Lambert, G. Noell, E. Schmaelzlin, K. Meerholz and C. Braeuchle, *Chem. Eur. J*., 1998, **4**, 2129.
119 X. Zhou, J.-K. Feng and A.-M. Ren, *Synth. Met*., 2005, **155**, 615.
120 a) H. Zhou, X. Zhao, T. Huang, R. Lu, H. Zhang, X. Qi, P. Xue, X. Liu and X. Zhang, *Org. Biomol. Chem*., 2011, **9**, 1600; b) L.-J. Gong, Y.-H. Wang, Z.-H. Kang, T.-H. Huang, R. Lu and H.-Z. Zhang, *Chin. J. Chem. Phys*., 2012, **25**, 636.
121 a) C. Ka Man Chan, C.-H. Tao, H.-L. Tam, N. Zhu, V. Wing-Wah Yam and K.-W. Cheah, *Inorg. Chem*., 2009, **48**, 2855; b) C. Ka Man Chan, C.-H. Tao, K.-F. Li, K. Man-Chung Wong, N. Zhu, K.-W. Cheah and V. Wing-Wah Yam, *J. Organomet. Chem*., 2011, **696**, 1163.
122 X.-B. Mao, Z. Ma, Y.-L. Yang, S.-B. Lei, C. Wang and W. Huang, *Front. Mater. Sci. China*, 2008, **2**, 26.
123 a) B. Such, T. Trevethan, T. Glatzel, S. Kawai, L. Zimmerli, E. Meyer, A.L. Shluger, C.H.M. Amijs, P. de Mendoza and A.M. Echavarren, *ACS Nano*, 2010, **4**, 3429; b) T. Trevethan, B. Such, T. Glatzel, S. Kawai, A.L. Shluger, E. Meyer, P. de Mendoza and A.M. Echavarren, *Small*, 2011, **7**, 1264.
124 R.S. Sprick, A. Thomas and U. Scherf, *Polym. Chem*., 2010, **1**, 283.
125 Q.Z. Ni, E. Daviso, T.V. Can, E. Markhasin, S.K. Jawla, T.M. Swager, R.J. Temkin, J. Herzfeld and R.G. Griffin, Acc. Chem. Res. 2013, **46**, 1933.
126 T. Maly, G.T. Debelouchina, V.S. Bajaj, K.-N. Hu, C.-G. Joo, M.L. Mak-Jurkauskas, J.R. Sirigiri, P.C.A. van der Wel, J. Herzfeld, R.J. Temkin and R.G. Griffin, *J. Chem. Phys*., 2008, **128**, 052211.
127 D.K. Frantz, J.J. Walish and T.M. Swager, *Org. Lett*., 2013, **15**, 4782.